The white-footed deermouse, an infection tolerant reservoir for several zoonotic agents, tempers interferon responses to endotoxin in comparison to the mouse and rat

Ana Milovic
Department of Microbiology & Molecular Genetics
University of California Irvine

Jonathan V. Duong
Department of Microbiology & Molecular Genetics
University of California Irvine

Alan G. Barbour[1]
Departments of Microbiology & Molecular Genetics, Medicine,
and Ecology & Evolutionary Biology
University of California Irvine
[1] Correspondence: abarbour@uci.ed

Abstract
The white-footed deermouse *Peromyscus leucopus*, a long-lived rodent, is a key reservoir for agents of several zoonoses, including Lyme disease. While persistently infected, this deermouse is without apparent disability or diminished fitness. For a model for inflammation elicited by various pathogens, the endotoxin lipopolysaccharide (LPS) was used to compare genome-wide transcription in blood by *P. leucopus*, *Mus musculus* and *Rattus norvegicus* and adjusted for white cell concentrations. Deermice were distinguished from the mice and rats by LPS response profiles consistent with non-classical monocytes and alternatively-activated macrophages. LPS-treated *P. leucopus*, in contrast to mice and rats, also displayed little transcription of interferon-gamma and lower magnitude fold-changes in type 1 interferon-stimulated genes. This was associated with comparatively reduced transcription of endogenous retrovirus sequences and cytoplasmic pattern recognition receptors in the deermice. The results reveal a mechanism for infection tolerance in this species and perhaps other animal reservoirs for agents of human disease.

Keywords
lipopolysaccharide | innate immune responses | interferon gamma | interferon type 1 | interferon-stimulated genes | endogenous retroviruses | PAMP triggered immunity | toll like receptor | neutrophil | monocyte | macrophage | Lyme disease

INTRODUCTION

How does the white-footed deermouse *Peromyscus leucopus* continue to thrive while sustaining infections with disease agents it serves as reservoir for (Barbour 2017)? The diverse tickborne pathogens (and diseases) for humans include the extracellular bacterium *Borreliella burgdorferi* (Lyme disease), the intracellular bacterium *Anaplasma phagocytophilum* (anaplasmosis), the protozoan *Babesia microti* (babesiosis), and the Powassan flavivirus (viral encephalitis). Most deermice remain persistently infected but display scant inflammation in affected tissues (Moody et al. 1994; Cook and Barbour 2015; Long et al. 2019), and without apparent consequence for fitness (Schwanz et al. 2011; Voordouw, Lachish, and Dolan 2015).

A related question—conceivably with the same answer--is what accounts for the two-to-three fold longer life span for *P. leucopus* than for the house mouse, *Mus musculus* (Sacher and Hart 1978; Labinskyy et al. 2009)? The abundance of *P. leucopus* across much of North America (Hall 1979; Moscarella et al. 2019) and its adaptation to a variety of environments, including urban areas and toxic

waste sites (Biser et al. 2004; Levengood and Heske 2008; Munshi-South and Kharchenko 2010), indicates successful adjustment to changing landscapes and climate. *Peromyscus* species, including the hantavirus reservoir *P. maniculatus* (Morzunov et al. 1998), are more closely related to hamsters and voles in family Cricetidae than to mice and rats of family Muridae (Bradley et al. 2014).

As a species native to North America, *P. leucopus* is an advantageous alternative to the house mouse, which is of Eurasian origin, for study of natural variation in populations that are readily at-hand (Bedford and Hoekstra 2015; Long et al. 2022). A disadvantage is the limited reagents and genetic tools of the sorts that are applied for mouse studies. As an alternative, we study *P. leucopus* with a non-reductionist approach that is comparative in design and agnostic in assumptions (Balderrama-Gutierrez et al. 2021). The genome-wide expression comparison for *P. leucopus* is with *M. musculus* and, added here, the brown rat *Rattus norvegicus*. Given the wide range of pathogenic microbes that deermice tolerate, we use the bacterial endotoxin lipopolysaccharide (LPS) as the primary experimental treatment because the inflammation it elicits within a few hours has features common to different kinds of serious infections, not to mention severe burns and critical injuries (Xiao et al. 2011).

We previously reported that a few hours after injection of LPS, *P. leucopus* and *M. musculus* had distinguishing profiles of differentially expressed genes (DEG) in the blood, spleen, and liver (Balderrama-Gutierrez et al. 2021). In brief, the inflammation phenotype of deermice was consistent with an "alternatively-activated" or M2-type macrophage polarization phenotype instead of the expected "classically-activated" or M1-type polarization phenotype that was observed for *M. musculus* (Murray et al. 2014). The deermice also differed from mice in displaying evidence of greater neutrophil activation and degranulation after LPS exposure. The potentially damaging action from neutrophil proteases and reactive oxygen species appeared to be mitigated in part in *P. leucopu*s by proteins like secretory leukocyte protease inhibitor (Slpi) and superoxide dismutase 2 (Sod2).

Here, we first address whether the heightened transcription of neutrophil-associated genes in *P. leucopus* is attributable to differences in numbers of white cells in the blood. To better match for genetic diversity, we substituted outbred *M. musculus* for the inbred BALB/c mouse of the previous study. We retained the experimental protocol of short-term responses to LPS. This main experiment was supplemented by a study of rats under the similar conditions and by an investigation of a different dose of LPS and duration of exposure in another group of deermice. The focus was on the blood of these animals, not only because the distinctions between species in their transcriptional profiles were nearly as numerous for this specimen as for spleen and liver (Balderrama-Gutierrez et al. 2021), but also because for ecological and immunological studies of natural populations of *Peromyscus* species blood is obtainable from captured-released animals without their sacrifice.

The results inform future studies of *Peromyscus* species, not only with respect to microbial infections and innate immunity, but also determinants of longevity and resilience in the face of other stressors, such as toxic substances in the environment. The findings pertain as well to the phenomenon of infection tolerance broadly documented in other reservoirs for human disease agents, such as betacoronaviruses and bats (Mandl et al. 2018). Less directly, the results provide for insights about maladaptive responses among humans to microbes, from systemic inflammatory response syndrome (SIRS) to post-infection fatigue syndromes.

RESULTS

LPS experiment and hematology studies.

Twenty adult animals of each species and equally divided between sexes received by intraperitoneal injection either purified *E. coli* LPS at a dose of 10 μg per g body mass or saline alone (Table 1). Within 2 h LPS-treated animals of both species displayed piloerection and sickness behavior, i.e. reduced activity, hunched posture, and huddling. By the experiment's termination at 4 h, 8 of 10 *M. musculus* treated with LPS had tachypnea, while only one of ten LPS-treated *P. leucopus* displayed this sign of the sepsis state ($p = 0.005$).

Table 1. Characteristics and treatments of *Mus musculus* CD-1 and *Peromyscus leucopus* LL stock

Animal	Genus	Sex	Age (d)	Mass (g)	Treatment	Tachypnea	Hct * (%)	MCV *	WBC *	Neutrophils	Lymphocytea	Monocytes	Eosinophils	Neutrophil/ Lymphocyte
MM19	*Mus*	female	149	60.4	control	no	71	62	3800	570	2926	190	114	0.19
MM21	*Mus*	female	149	51.4	control	no	51	59	8600	826	4897	177	0	0.17
MM23	*Mus*	female	149	30.6	control	no	51	.	1500	135	1305	60	0	0.10
MM25	*Mus*	female	149	42.1	control	no	65	61	7900	1106	6557	237	0	0.17
MM27	*Mus*	female	149	39.7	control	no	58	62	3700	962	2257	333	148	0.43
MM1	*Mus*	male	149	50.9	control	no	67	59	3300	726	2376	198	0	0.31
MM17	*Mus*	male	149	40.8	control	no	51	.	7000	4970	2030	0	0	2.45
MM3	*Mus*	male	149	45.8	control	no	58	59	4300	344	3655	301	0	0.09
MM5	*Mus*	male	149	41.2	control	no	60	57	5400	810	4266	324	0	0.19
MM7	*Mus*	male	149	44.1	control	no	47	58	3800	798	2736	266	0	0.29
MM31	*Mus*	female	149	65.5	LPS	yes	53	58	1900	209	1539	114	38	0.14
MM33	*Mus*	female	149	48.4	LPS	yes	62	62	3200	256	2784	96	64	0.09
MM35	*Mus*	female	149	40.5	LPS	yes	49	64	2200	528	1518	88	66	0.35
MM37	*Mus*	female	149	38.5	LPS	no	54	65	1900	152	1634	57	57	0.09
MM39	*Mus*	female	149	40.2	LPS	yes	61	63	600	60	510	12	18	0.12
MM11	*Mus*	male	149	57.4	LPS	yes	59	58	2600	572	1898	104	0	0.30
MM13	*Mus*	male	149	58.5	LPS	yes	66	59	3700	1258	2183	259	0	0.58
MM15	*Mus*	male	149	51.0	LPS	yes	33	56	1800	90	1602	90	0	0.06
MM29	*Mus*	male	149	39.1	LPS	no	53	59	1800	306	1368	72	54	0.22
MM9	*Mus*	male	149	44.1	LPS	yes	58	.	1300	260	858	182	0	0.30
24841	*Peromyscus*	female	162	19.9	control	no	58	48	5100	204	4590	102	204	0.04
24842	*Peromyscus*	female	164	18.3	control	no	47	48	3900	663	3003	117	117	0.22
24843	*Peromyscus*	female	162	20.5	control	no	45	46	4200	942	3150	42	84	0.30
24845	*Peromyscus*	female	161	18.7	control	no	49	48	9100	2002	6916	182	0	0.29
24853	*Peromyscus*	female	160	22.8	control	no	42	.	4800	1008	2880	864	1	0.35
24852	*Peromyscus*	male	162	19.4	control	no	44	46	7100	994	4970	284	852	0.20
24861	*Peromyscus*	male	157	20.8	control	no	28	50	1300	104	1053	91	52	0.10
24863	*Peromyscus*	male	157	17.1	control	no	26	58	7200	720	5904	288	288	0.12
24869	*Peromyscus*	male	143	29.0	control	no	48	52	6000	1260	4260	180	240	0.30
24876	*Peromyscus*	male	142	16.1	control	no	54	48	9700	2716	6208	194	485	0.44
24846	*Peromyscus*	female	162	22.7	LPS	no	23	47	1100	231	718	44	44	0.32
24847	*Peromyscus*	female	162	16.7	LPS	no	39	.	1500	570	675	180	75	0.84
24848	*Peromyscus*	female	166	16.2	LPS	no	43	49	2700	918	1701	27	54	0.54
24850	*Peromyscus*	female	157	19.4	LPS	no	46	.	3300	1551	1683	66	0	0.92
24851	*Peromyscus*	female	161	25.4	LPS	no	24	47	2300	552	1242	437	69	0.44
24855	*Peromyscus*	male	165	27.1	LPS	no	51	51	2100	1281	714	42	63	1.79
24860	*Peromyscus*	male	160	17.8	LPS	yes	42	54	13200	6996	3696	1320	1056	1.89
24865	*Peromyscus*	male	160	16.7	LPS	no	49	46	1800	396	1080	288	0	0.37
24873	*Peromyscus*	male	145	23.2	LPS	no	43	48	2200	550	1430	110	110	0.38
24879	*Peromyscus*	male	145	22.0	LPS	no	40	.	1100	220	538	352	0	0.41

* Abbreviations: Hct, hematocrit; MCV, mean cellular volume of erythrocytes; WBC, white blood cell count

Within a given species there was little difference between LPS-treated and control animals in values for erythrocytes. But overall the deermice had lower mean (95% confidence interval) hematocrit at 42% (36-48), hemoglobin concentration at 13.8 g/dL (12.1-15.5), and mean corpuscular volume for erythrocytes at 49 fL (47-51) than *M. musculus* with respective values of 56% (51-62), 16.1 g/dL (14.6-17.7), and 60 fL (58-62) ($p < 0.01$). These hematology values for adult CD-1 *M. musculus* and LL stock *P. leucopus* in this study were close to what had been reported for these colony populations (CharlesRiver 2012; Wiedmeyer et al. 2014).

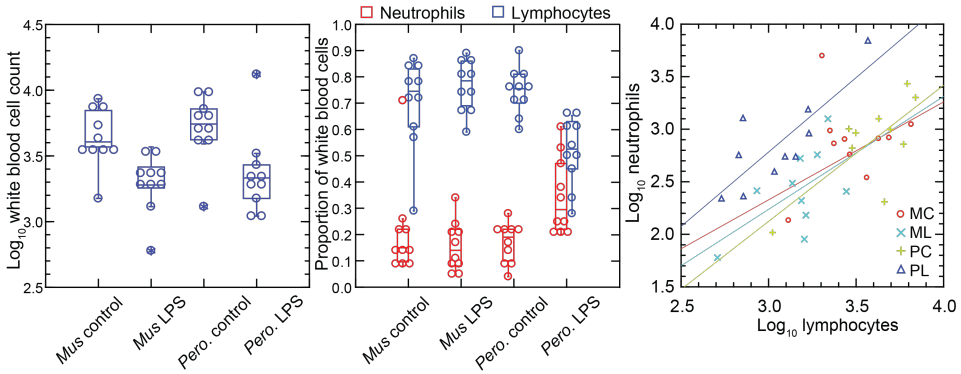

Figure 1. Total white blood cells, neutrophils, and lymphocytes of *Mus musculus* (M) and *Peromyscus leucopus* (P) with or without (control; C) treatment with 10 µg lipopolysaccharide (LPS; L) per g body mass 4 h previous. The box plots of left and center panels show values of individual animals and compile median, quartiles, and extreme values. The linear regressions of the right panel are color-coded according to the species and treatment designations. The outlier value for a *M. musculus* control was excluded from the linear regression for that group.

In contrast to red blood cells, the mean numbers of white blood cells in the LPS groups in both species were lower than those of control groups (Figure 1). Controls had a mean 4.9 (3.5-6.4) x 10^3 white cells per μl among *M. musculus* and 5.8 (4.2-7.4) x 10^3 white cells per μl among *P. leucopus* (p = 0.41). For the LPS-treated animals the values were 2.1 (1.5-2.7) x 10^3 for mice and 3.1 (0.9-5.4) x 10^3 for deermice (p = 0.39). However, there was difference between species among LPS-treated animals in the proportions of neutrophils and lymphocytes in the white cell population. The ratios of neutrophils to lymphocytes were 0.25 (0.14-0.45) and 0.20 (0.13-0.31) for control *M. musculus* and *P. leucopus*, respectively (p = 0.53). But under the LPS condition. the neutrophil-to-lymphocyte ratio was 0.18 (0.11-0.28) for mice and 0.64 (0.42-0.97) for deermice (p = 0.0006). The regression curves for plots of neutrophils and lymphocytes for LPS-treated and control *P. leucopus* and LPS-treated *M. musculus* had similar slopes, but the y-intercept was shifted upwards towards a higher ratio of neutrophils to lymphocytes for blood from the LPS group of deermice. Control group mice and deermice and LPS-treated mice had similar percentages (~5%) of monocytes in their blood; the mean monocyte percentage rose to 10% in LPS treated deermice (p = 0.12). Eosinophil percentages tended to be higher in deermice at a mean 3.4 (2.1-4.7)% than mice at 1.2 (0.5-1.9)% under either condition (p = 0.004).

In the *P. leucopus* experiment with a 10-fold lower dose of LPS and a 12 hour duration, the mean (95% confidence interval) white blood cell count (x 10^3) at termination 3.5 (2.5-4.5) in controls and 7.9 (6.0-9.7) in the LPS-treated (p = 0.01). Even with the higher overall white blood cell count the increase white cells was proportionately higher for neutrophils than for lymphocytes, as was seen in the deermice in the higher dose LPS experiment. The ratio of neutrophils-to-lymphocytes was 0.20 (0.07-0.32) in the controls and 0.38 (0.26-0.50) (p = 0.10).

The higher neutrophil to lymphocyte ratio in the deermice exposed to LPS was consistent with the greater neutrophil activation noted by transcriptional analysis (Balderrama-Gutierrez et al. 2021). But many individual genes that constitute this and related gene ontology (GO) terms had transcription levels in the deermice that far exceeded a three-fold difference in neutrophil counts. For some genes fold-changes were a hundred or more fold, which suggested that the distinctive LPS transcriptional response profile between species was not attributable solely to neutrophil counts.

Genome-wide expression in blood of deermice and mice

We used the respective transcript sets from the reference genomes for *P. leucopus* and *M. musculus* for deep coverage RNA-seq with paired-end ~150 nt reads. Principle component analyses (PCA) of the *P. leucopus* data and *M. musculus* data revealed that untreated controls had coherent profiles within each species (Figure 2). With the exception of one mouse, the LPS-treated *M. musculus* were also in a tight PCA cluster. In contrast, the LPS-treated deermice displayed a diversity of genome-wide transcription profiles and limited clustering.

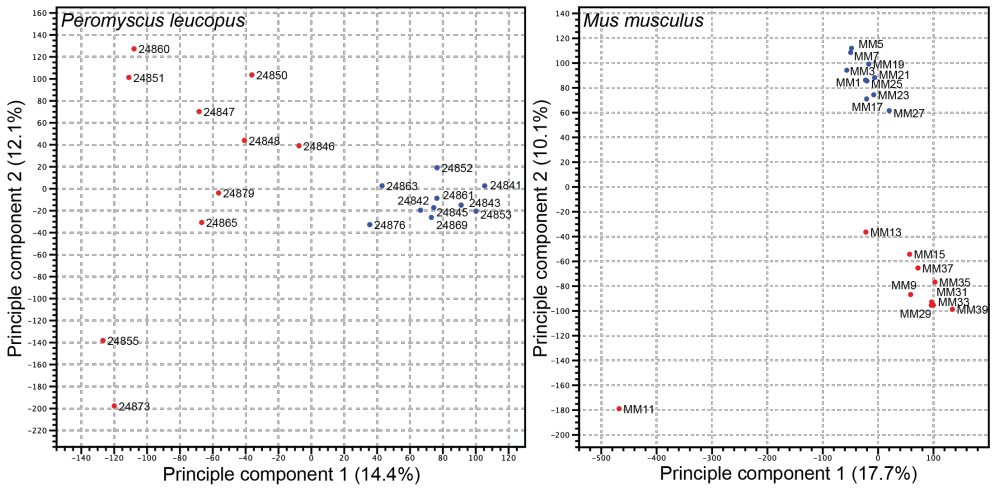

Figure 2. Principle component analysis of genome-wide RNA-seq data of *P. leucopus* or *M. musculus* with (red dot) or without (blue dot) treatment with LPS 4 h previous. The individual animals listed in Table 1 are indicated on the graphs.

For both species the number of genes with higher expression with LPS exposure exceeded those with lower or unchanged expression (Dryad Table D1). For *P. leucopus* and *M. musculus* the mean fold-changes were 1.32 (1.29-1.35) and 1.30 (1.24-1.36), respectively ($p = 0.31$). Among *P. leucopus* 1154 DEGs with an absolute fold-change ≥ 2 and false-discovery rate p value < 0.003 were identified. The corresponding number for *M. musculus* was 1266. Two DEGs that distinguished females from males among controls or LPS-treated were the non-coding Xist, the X chromosome inactivating gene, for females and the Y chromosome-linked DEAD-box helicase 3 (Ddx3y) gene for males.

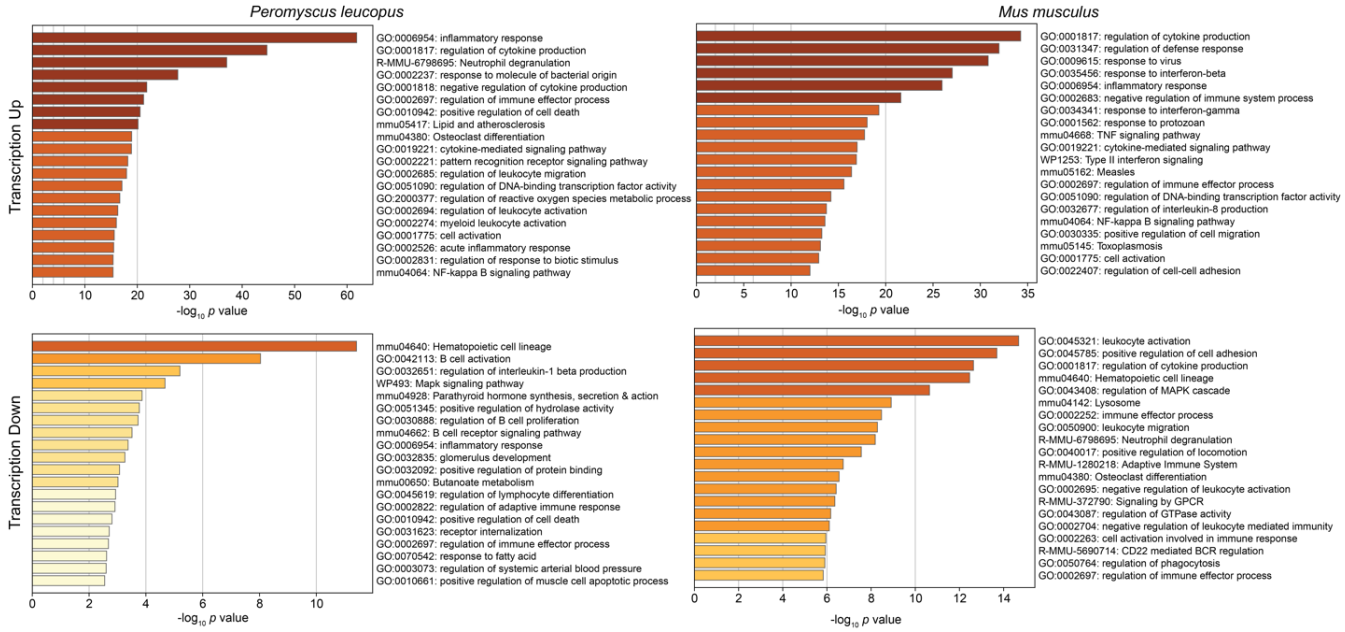

Figure 3. Gene Ontology (GO) terms associated with up-regulated genes (upper panels) and down-regulated genes (lower panels) of *P. leucopus* and *M. musculus* treated with LPS in comparison with untreated controls of each species.

Figure 3 shows the GO term analyses of these DEGs for *P. leucopus* and *M. musculus*. The up-regulated gene profile for *P. leucopus* featured GO terms associated with "neutrophil degranulation", "myeloid leukocyte activation", "leukocyte migration", and "response to molecule of bacterial origin". Other sets of up-regulated genes for the deermice were "negative regulation of cytokine production" and "regulation of reactive oxygen species metabolic process". None of these were up-regulated gene GO terms with p values < 10^{11} for *M. musculus*. Indeed, "leukocyte activation" and "leukocyte migration" were GO terms for down-regulated DEGs in *M. musculus*. Distinctive GO terms for up-regulated genes distinguishing mice from deermice were "response to virus", "response to interferon-beta", "response to interferon-gamma", "response to protozoan", and "type II interferon signaling".

Of the top 100 DEGs for each species by ascending FDR p value, 24 genes were shared between species (Supplementary Materials Table S1). These included up-regulated Bcl3, Ccl3, Cxcl1, Cxcl2, Cxcl3, Cxcl10, Il1rn, and Sod2. Among the 100 mouse DEGs, 20 were constituents of GO terms "response to virus" (GO:0009615) or "response to interferon-beta" (GO:0035456) and only 3 were members of GO term sets "response to molecule of bacterial origin" (GO:0002237) or "response to lipopolysaccharide" (GO:0032496). In contrast, among the top 100 deermouse DEGs, there were only 2 associated with the virus or type 1 interferon GO terms, but 12 were associated with either or both of the bacterial molecule GO terms.

The emerging picture was of *P. leucopus* responding to LPS exposure as if infected with an extracellular bacterial pathogen, including with activated neutrophils. While *M. musculus* animals shared with *P. leucopus* some features of an antibacterial response, they also displayed type I and type II interferon type response profiles associated with infections with viruses and intracellular bacteria and parasites.

Targeted RNA seq analysis

A challenge for cross-species RNA-seq is commensurability between annotated transcripts of reference sets. Orthologous genes can be identified, but mRNA isoforms and their 5′ and 3′ untranslated regions may not fully correspond. Accordingly, we limited targeted RNA-seq to protein coding sequences of mRNAs for the corresponding sets of *P. leucopus* and *M. musculus* sequences.

For cross-species normalization we chose a gene whose transcription approximated the varying numbers of white cells. The myeloid cell marker CD45, formally "protein tyrosine phosphatase, receptor type, C", and encoded by the Ptprc gene, was the denominator transcript for normalization across species and treatments. In humans, mice, and hamsters, Ptprc is expressed by nucleated hematopoietic cells and used as a white cell marker for flow cytometry (Schnizlein-Bick et al. 2002). Pearson's continuous and Spearman's ranked correlations between log-transformed total white blood cell counts and normalized reads for Ptprc across 40 animals representing both species, sexes, and treatments were 0.40 ($p = 0.01$) and 0.34 ($p = 0.03$), respectively.

The 113 mRNA coding sequences, which are listed in Methods, were drawn from the identified DEGs for *P. leucopus* and *M. musculus* from the genome-wide RNA-seq. Figure 4 comprises plots of the log-transformed mean target-to-Ptprc ratios for the 10 *P. leucopus* controls and 10 *M. musculus* controls (left panel) and for the 10 *P. leucopus* and 10 *M. musculus* treated with LPS (right panel). For untreated animals there was high correlation and a regression coefficient of ~1 between the paired data for deermice and mice. The mitochondrial cytochrome oxidase 1 gene (MT-Co1) and S100a9, a subunit of calprotectin, were comparably transcribed. But, there were other coding sequences that stood out for either their greater or lesser transcription in untreated deermice than mice. Two examples of greater expression were Arg1 and MX dynaminin-like GTPase 2 (Mx2), an ISG, while two examples of lesser expression were matrix metalloprotease 8 (Mmp8) and Slpi. There was low to undetectable transcription of Nos2 and interferon-gamma (Ifng) in the blood of controls of both species.

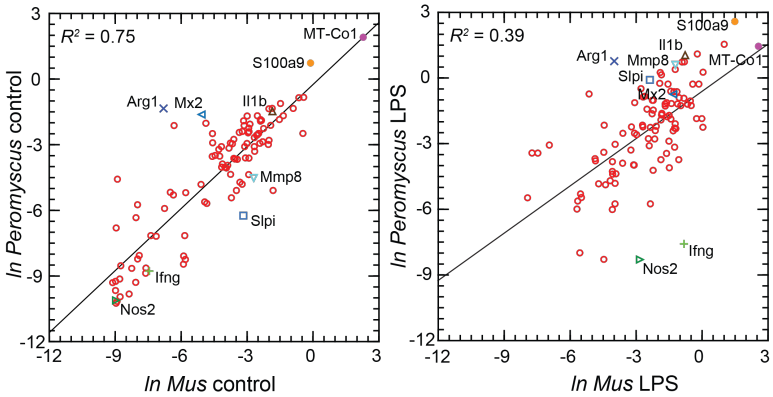

Figure 4. Scatter plots with linear regression of pairs of log-transformed (*ln*) normalized RNA-seq reads for selected coding sequences for control *P. leucopus* and *M. musculus* (left panel) and LPS-treated *P. leucopus* and *M. musculus* (right panel). The coefficients of determination (R^2) and selected genes (each by a different symbol) are indicated in each graph.

For the LPS-treated animals there was, as expected for this selected set, higher expression of the majority genes and greater heterogeneity between *P. leucopus* and *M. musculus* in their responses for represented genes. In contrast to the findings with controls, Ifng and Nos2 were substantially more transcribed in treated mice, but these genes were only marginally so in deermice. A comparatively restrained transcriptional response in deermice was also noted for Mx2. On the other hand, there were greater fold-change from baseline in *P. leucopus* than in *M. musculus* for interleukin-1 beta (Il1b), Mmp8, Slpi, and S100a9.

Table 2 lists all the selected targets with the means and confidence intervals for the normalized values for controls and LPS-treated *M. musculus* and controls and LPS-treated *P. leucopus*, as well as the fold-changes within each species and between treatments.The values for individual animals by species, sex, and treatment are provided in Supplementary Materials Table S2. In Table 2. The final column is the ratio of the fold-change between LPS to control in *P. leucopus* to the corresponding value for *M. musculus*. This along with the derived heat-map of these ratios, which presented in the second column, indicates the genes for which there was little difference between species in their responses to LPS--

either up or down--as well as those that were comparatively greater or lesser in one species or the other. Several of these genes are considered in other specific contexts below.

Table 2. Targeted RNA-seq of blood of *Peromyscus leucopus* and *Mus musculus* 4 hours after intraperitoneal injection of lipopolysaccharide (LPS) or saline control

Gene *	Heatmap †	Mus control mean (95% CI) ‡	Mus LPS mean (95% CI)	Mus FC LPS vs control**	Mus FDR p value**	Peromyscus control mean (95% CI)	Peromyscus LPS mean (95% CI)	Peromyscus FC LPS v control	Peromyscus FDR p value	Peromyscus v Mus control FC	Peromyscus v Mus LPS FC	Peromyscus v Mus LPS/control †
Ibsp		0.51 (0.28-0.93)	5.99 (2.04-17.6)	11.7	2E-03	0.17 (0.06-0.47)	471 (305-728)	2720	3E-10	0.34	78.6	233
Slpi		42.0 (32.6-54.0)	93.2 (44.5-195)	2.22	7E-02	1.94 (0.96-3.94)	921 (636-1333)	474	1E-10	0.05	9.88	213
Steap1		0.13 (0.10-0.16)	0.58 (0.21-1.60)	4.52	1E-02	0.09 (0.05-0.17)	31.7 (16.3-61.4)	335	1E-09	0.73	54.3	74.2
Saa3		2.82 (0.89-8.95)	458 (165-1267)	162	7E-06	0.21 (0.12-0.37)	2052 (1273-3306)	9934	2E-13	0.07	4.48	61.2
Lpo		0.13 (0.09-0.20)	0.37 (0.19-0.72)	2.78	2E-02	0.03 (0.03-0.04)	4.10 (1.44-11.7)	118	1E-07	0.26	11.2	42.4
Mmp8		67.4 (34.3-133)	298 (187-477)	4.43	3E-03	10.9 (4.26-27.8)	1823 (1311-2534)	168	3E-08	0.16	6.11	37.9
Lrg		40.8 (22.1-75.3)	107 (52.2-219)	2.62	7E-02	8.01 (2.98-21.5)	353 (268-464)	44.1	2E-06	0.20	3.30	16.8
Mmp9		222 (147-335)	153 (90.1-258)	0.69	3E-01	154 (96.8-245)	1258 (903-1753)	8.17	2E-06	0.69	8.25	11.9
Csf3		0.14 (0.10-0.19)	7.85 (3.07-20.1)	57.1	6E-07	0.04 (0.03-0.05)	24.5 (8.95-67.1)	648	2E-09	0.27	3.12	11.4
Serpine1		0.51 (0.27-0.93)	11.7 (3.04-45.2)	23.2	9E-04	0.14 (0.06-0.32)	32.8 (4.82-223)	239	9E-05	0.27	2.80	10.3
Fpr2		36.9 (25.8-52.7)	246 (168-362)	6.68	2E-06	8.74 (6.48-11.8)	535 (399-717)	61.2	5E-12	0.24	2.17	9.16
Cxcl3		0.32 (0.17-0.59)	19.6 (12.3-31.3)	60.8	2E-08	0.09 (0.04-0.21)	47.2 (15.9-140)	523	2E-07	0.28	2.41	8.59
Retn		0.35 (0.18-0.68)	0.45 (0.26-0.77)	1.28	6E-01	3.13 (1.80-5.46)	31.8 (22.0-45.9)	10.1	4E-06	8.96	71.1	7.93
Csf3r/Cd114		669 (455-982)	302 (221-411)	0.45	7E-03	423 (318-563)	1445 (1024-2040)	3.42	6E-05	0.63	4.79	7.58
Fcgr3/Cd16		45.7 (31.7-65.8)	70.1 (35.1-140)	1.53	3E-01	44.7 (34.1-58.6)	409 (338-497)	9.17	1E-09	0.98	5.84	5.97
Pfx		0.24 (0.17-0.33)	4.06 (0.94-17.6)	17.0	2E-03	0.05 (0.03-0.09)	4.88 (1.10-21.6)	92.2	4E-05	0.22	1.20	5.42
Fcgr2a		78.8 (59.1-105)	149 (93.8-237)	1.89	4E-02	75.0 (62.0-90.8)	766 (597-983)	10.2	2E-10	0.95	5.14	5.40
Cd177		25.0 (11.1-56.1)	158 (80.2-310)	6.31	4E-03	4.29 (2.12-8.69)	144 (107-194)	33.5	1E-07	0.17	0.91	5.31
Ncf4		134 (112-160)	204 (172-242)	1.52	5E-03	49.1 (38.4-62.9)	317 (258-389)	6.46	5E-09	0.37	1.55	4.24
Il1b		158 (102-244)	464 (341-631)	2.94	1E-03	230 (146-362)	2845 (1998-4052)	12.4	2E-07	1.45	6.14	4.22
Fcgr2b		32.7 (27.4-39.0)	111 (78.2-156)	3.38	1E-05	24.9 (22.4-27.8)	352 (302-409)	14.1	2E-14	0.76	3.18	4.17
Hk3		35.8 (25.7-50.0)	63.6 (46.6-86.8)	1.78	3E-02	85.5 (66.8-109)	602 (468-773)	7.04	1E-08	2.39	9.46	3.96
Fgr		138 (110-174)	161 (125-207)	1.17	4E-01	251 (205-308)	1131 (987-1295)	4.50	3E-09	1.82	7.02	3.85
Tlr4		11.9 (8.62-16.4)	11.9 (6.23-22.8)	1.00	1E+00	29.7 (22.9-38.6)	113 (90.7-141)	3.81	1E-06	2.50	9.49	3.80
Glrx		54.8 (43.1-69.7)	122 (65.4-227)	2.22	4E-02	12.4 (11.1-13.9)	88.4 (71.6-109)	7.11	5E-11	0.23	0.73	3.20
Slc11a1/Nramp		54.9 (41.6-72.5)	75.3 (60.0-94.6)	1.37	1E-01	104 (88.0-123)	424 (308-582)	4.07	1E-06	1.89	5.62	2.97
Ccl3		3.07 (2.20-4.30)	227 (161-320)	73.9	2E-11	0.26 (0.14-0.48)	54.6 (33.2-89.8)	213	1E-09	0.08	0.24	2.88
Tlr1		71.8 (63.3-81.5)	52.2 (37.4-72.8)	0.73	1E-01	36.0 (29.8-43.4)	73.3 (61.6-87.1)	2.04	5E-05	0.50	1.40	2.81
Hmox1		16.0 (12.5-20.6)	27.8 (13.7-56.7)	1.74	2E-01	17.4 (14.9-20.4)	78.2 (51.5-119)	4.49	6E-06	1.09	2.81	2.58
Tnfrsf1a		70.8 (57.2-87.7)	69.3 (45.5-106)	0.98	9E-01	44.6 (34.1-58.4)	105 (89.0-123)	2.34	6E-05	0.63	1.51	2.40
Olfm4		7.41 (3.43-16.0)	162 (98.8-266)	21.9	6E-06	3.56 (1.96-6.44)	181 (101-326)	51.0	1E-07	0.48	1.12	2.33
Sod2		58.1 (48.3-69.9)	412 (262-650)	7.10	8E-07	124 (80.5-192)	2030 (1666-2475)	16.3	5E-09	2.14	4.92	2.30
Il2ra/Cd25		12.3 (3.95-38.3)	8.23 (3.06-22.2)	0.67	6E-01	4.33 (3.80-4.94)	5.77 (4.38-7.61)	1.33	9E-02	0.35	0.70	1.99
Lcn2		29.6 (14.9-58.9)	2797 (1832-4271)	94.5	1E-08	25.2 (11.4-55.9)	4571 (3268-6393)	181	3E-09	0.85	1.63	1.92
Sting		51.2 (42.7-61.3)	47.8 (38.5-59.3)	0.93	7E-01	181 (160-204)	317 (277-363)	1.76	2E-05	3.53	6.64	1.88
Jak2		166 (150-185)	355 (267-472)	2.13	2E-04	6.02 (5.43-6.66)	23.4 (16.5-33.2)	3.89	2E-06	0.04	0.07	1.82
Lrrk2		93.9 (82.2-107)	83.5 (66.1-105)	0.89	4E-01	153 (125-188)	236 (163-340)	1.54	6E-02	1.63	2.82	1.73
Il1rn		18.6 (12.1-28.6)	325 (185-572)	17.5	7E-07	17.4 (13.0-23.3)	523 (408-670)	30.0	2E-11	0.94	1.61	1.72
Csf1		8.18 (5.53-12.1)	17.5 (12.0-25.5)	2.14	2E-02	3.32 (2.43-4.55)	12.1 (8.04-18.1)	3.63	1E-04	0.41	0.69	1.70
Cfb		6.28 (4.26-9.25)	111 (46.0-269)	17.7	2E-05	7.93 (3.52-17.9)	225 (140-362)	28.4	3E-06	1.26	2.03	1.60
Itgam/Cd11b		265 (207-339)	361 (283-461)	1.37	1E-01	183 (135-250)	396 (278-564)	2.16	5E-03	0.69	1.10	1.58
Timp1		108 (94.0-124)	192 (117-316)	1.78	5E-02	102 (91.0-114)	272 (226-326)	2.67	1E-07	0.94	1.41	1.50
Socs3		19.9 (12.8-30.8)	254 (213-304)	12.8	2E-08	16.8 (12.1-23.4)	304 (224-413)	18.1	1E-09	0.84	1.20	1.42
Il6		0.27 (0.17-0.42)	9.27 (5.27-16.3)	34.5	5E-08	0.17 (0.09-0.33)	7.77 (1.74-34.6)	45.5	3E-04	0.64	0.84	1.32
Ltf		10.5 (5.82-18.8)	824 (445-1526)	78.8	3E-08	28.5 (12.0-68.0)	2930 (2069-4151)	103	5E-08	2.73	3.56	1.30
S100a9		912 (539-1543)	4540 (2426-8497)	4.98	2E-03	2036 (1240-3344)	12972 (10079-16695)	6.37	6E-06	2.23	2.86	1.28
Cxcl1		0.13 (0.09-0.19)	20.3 (9.03-45.7)	158	9E-09	0.06 (0.03-0.13)	12.3 (3.08-49.0)	198	6E-06	0.48	0.60	1.25
Il10		0.11 (0.10-0.13)	3.57 (1.86-6.87)	31.7	3E-08	0.09 (0.05-0.15)	3.53 (1.13-11.0)	39.6	3E-05	0.79	0.99	1.25
Gapdh		646 (591-707)	1014 (558-1845)	1.57	2E-01	667 (590-754)	1295 (923-1818)	1.94	2E-03	1.03	1.28	1.24
Csf1r/Cd115		233 (201-270)	47.3 (31.7-70.7)	0.20	2E-06	320 (262-390)	78.3 (44.7-137)	0.24	2E-04	1.37	1.66	1.21
Nfkb1		149 (133-168)	336 (283-399)	2.25	1E-06	118 (114-122)	300 (209-431)	2.54	1E-04	0.79	0.89	1.13
Nr3c1		124 (105-148)	119 (101-139)	0.95	7E-01	47.0 (41.5-53.1)	49.9 (38.3-65.2)	1.06	7E-01	0.38	0.42	1.11
Akt1		98.1 (82.8-116)	68.1 (54.1-85.7)	0.69	3E-02	148 (133-164)	113 (88.8-144)	0.76	6E-02	1.51	1.66	1.10
Pkm		538 (469-618)	884 (506-1544)	1.64	1E-01	417 (364-479)	741 (558-983)	1.77	2E-03	0.78	0.84	1.08
Il4ra/Cd124		91.2 (80.2-104)	247 (198-309)	2.71	1E-06	51.7 (47.2-56.7)	150 (122-184)	2.90	8E-08	0.57	0.61	1.07
Fcer2		104 (70.7-153)	15.7 (10.0-24.5)	0.15	1E-05	55.7 (47.6-65.1)	8.93 (4.96-16.1)	0.16	2E-05	0.54	0.57	1.06
Camp		3.12 (1.76-5.54)	285 (145-558)	91.2	3E-08	5.42 (2.26-13.0)	524 (354-776)	96.7	8E-08	1.74	1.84	1.06
Hif1a		53.4 (46.5-61.5)	191 (144-254)	3.58	8E-07	83.6 (77.0-90.8)	299 (203-440)	3.58	1E-05	1.56	1.57	1.00
Padi4		15.9 (8.70-29.0)	41.2 (22.3-76.0)	2.59	5E-02	44.6 (34.1-58.4)	105 (89.0-123)	2.34	6E-05	2.81	2.54	0.90
Bcl3		21.1 (14.8-30.0)	209 (168-260)	9.92	1E-08	18.9 (15.1-23.8)	167 (127-219)	8.80	3E-09	0.90	0.80	0.89
Mt2		0.38 (0.19-0.77)	89.1 (33.8-235)	235	1E-07	0.31 (0.13-0.75)	61.2 (20.5-182)	199	2E-06	0.81	0.69	0.84
Myd88		50.8 (39.5-65.4)	127 (96.0-168)	2.50	2E-04	51.5 (46.6-56.8)	108 (99.7-116)	2.09	5E-09	1.01	0.85	0.84
Thy1		35.0 (22.6-54.2)	25.2 (13.3-48.0)	0.72	5E-01	503 (457-553)	297 (240-368)	0.59	4E-04	14.4	11.8	0.82
Jun		31.4 (23.9-41.2)	157 (105-234)	5.01	6E-06	6.02 (5.43-6.66)	23.4 (16.5-33.2)	3.89	2E-06	0.19	0.15	0.78
Icam		24.1 (20.3-28.6)	301 (257-352)	12.5	3E-12	12.6 (10.5-15.0)	121 (67.3-217)	9.61	2E-06	0.52	0.40	0.77
Cx3cr1		27.9 (21.8-35.7)	3.46 (1.99-6.00)	0.12	4E-06	26.1 (19.0-35.9)	2.45 (1.44-4.15)	0.09	1E-06	0.94	0.71	0.76
Cxcl2		0.16 (0.09-0.26)	119 (76.0-186)	762	6E-12	0.10 (0.04-0.26)	60.2 (19.6-185)	574	2E-07	0.67	0.51	0.75
Akt2		138 (117-163)	275 (182-415)	1.99	9E-03	59.4 (57.1-61.7)	87.6 (71.5-107)	1.47	2E-03	0.43	0.32	0.74
Jak1		415 (386-447)	623 (467-830)	1.50	2E-02	256 (232-281)	277 (214-359)	1.09	6E-01	0.61	0.45	0.72
ERV Gag-pol		3210 (2406-4283)	13633 (10083-18433)	4.3	4E-06	233 (195-278)	692 (548-873)	2.97	2E-06	0.07	0.05	0.70
Pbib		93.7 (82.3-107)	97.2 (58.5-161)	1.04	9E-01	143 (134-153)	102 (71.2-147)	0.71	9E-02	1.53	1.05	0.69
Nox1		0.14 (0.11-0.18)	0.98 (0.65-1.48)	7.01	8E-07	10.1 (8.12-12.5)	45.6 (34.4-60.5)	4.53	3E-07	71.8	46.4	0.65
Tnf		2.99 (2.26-3.96)	19.5 (14.0-27.1)	6.52	3E-07	0.76 (0.42-1.40)	3.10 (1.62-5.95)	4.06	7E-03	0.26	0.16	0.62
Tlr2		26.1 (18.1-37.5)	165 (126-215)	6.31	6E-07	50.8 (37.2-69.5)	194 (128-294)	3.83	1E-04	1.95	1.18	0.61
Cd8		23.8 (19.6-29.0)	17.3 (13.6-22.1)	0.73	7E-02	52.6 (41.6-66.5)	21.3 (10.2-44.7)	0.41	4E-02	2.21	1.23	0.56
Stat1		160 (132-193)	449 (247-814)	2.81	6E-03	256 (221-297)	387 (323-465)	1.51	3E-03	1.60	0.86	0.54
Mapk1		71.1 (65.5-77.0)	92.6 (65.0-132)	1.30	2E-01	67.5 (63.9-71.3)	44.2 (37.4-52.3)	0.65	2E-04	0.95	0.48	0.50
Arg1		1.12 (0.36-3.42)	18.4 (5.99-56.7)	16.5	4E-03	261 (154-441)	2161 (1709-2732)	8.28	2E-06	234	117	0.50
Ccl2		0.16 (0.10-0.27)	12.7 (4.87-33.0)	77.7	8E-07	0.19 (0.07-0.50)	7.42 (3.23-17.0)	38.5	3E-05	1.18	0.58	0.50
Rigi/Ddx58		47.3 (41.9-53.3)	293 (175-491)	6.20	0.00	26.6 (20.5-34.4)	98.9 (76.9-127)	3.72	0.00	0.60	0.29	0.49
MT-Co1		10015 (7976-12576)	13316 (6322-28047)	1.33	5E-01	6608 (4976-8775)	4164 (2563-6765)	0.63	1E-01	0.66	0.31	0.47
Cd4		55.6 (45.7-67.6)	27.5 (19.6-38.8)	0.50	4E-03	88.5 (75.5-104)	19.9 (10.4-38.3)	0.23	5E-04	1.59	0.72	0.45
Socs1		0.82 (0.59-1.13)	45.4 (25.6-80.4)	55.6	3E-09	0.74 (0.53-1.04)	18.4 (9.19-36.9)	24.8	5E-07	0.91	0.41	0.45
Cd3d		81.9 (71.8-93.4)	46.7 (32.8-66.5)	0.57	1E-02	77.1 (64.1-92.7)	18.3 (8.91-37.6)	0.24	2E-03	0.94	0.39	0.42
Mtor		27.9 (24.3-31.9)	40.2 (34.9-46.3)	1.44	2E-03	62.1 (55.6-69.4)	36.3 (27.4-48.1)	0.58	3E-03	2.23	0.90	0.41
Il18		1.78 (1.18-2.70)	4.24 (2.84-6.32)	2.38	1E-02	4.89 (4.22-5.67)	4.15 (2.40-7.18)	0.85	6E-01	2.74	0.98	0.36
Stat2		41.0 (36.6-45.9)	229 (144-364)	5.59	2E-06	89.1 (75.3-105)	177 (153-206)	1.99	2E-05	2.17	0.77	0.36
Il7r/Cd127		36.8 (29.2-46.3)	39.6 (28.4-55.1)	1.08	7E-01	59.2 (50.5-69.3)	22.3 (15.5-32.0)	0.38	2E-04	1.61	0.56	0.35
Tgfb		0.13 (0.09-0.19)	8.02 (3.82-16.8)	60.6	4E-08	1.08 (0.78-1.50)	22.1 (11.5-42.5)	20.4	5E-07	8.18	2.76	0.34
Acod1		1.20 (0.60-2.37)	388 (289-521)	324	2E-10	2.64 (1.72-4.05)	276 (202-378)	105	2E-11	2.21	0.71	0.32
Csf2		0.16 (0.11-0.23)	3.94 (2.09-7.43)	24.9	3E-07	0.05 (0.03-0.07)	0.33 (0.11-0.98)	7.10	4E-03	0.29	0.08	0.28
Stat4		55.4 (50.4-60.8)	110 (95.3-128)	1.99	8E-07	26.4 (21.8-32.0)	14.4 (10.4-19.9)	0.55	6E-03	0.48	0.13	0.27
Dhx58/Lgp2		11.3 (9.76-13.2)	156 (77.1-317)	13.8	2E-06	20.2 (14.3-28.4)	73.1 (55.9-95.5)	3.63	3E-05	1.78	0.47	0.26
Isg15		81.5 (65.6-101)	600 (219-1646)	7.37	2E-03	183 (104-322)	342 (175-668)	1.87	2E-01	2.24	0.57	0.25
Oas1		10.6 (8.90-12.6)	106 (49.4-225)	9.98	3E-05	81.1 (51.9-127)	191 (127-285)	2.35	1E-02	7.67	1.81	0.24
Cgas		1.55 (1.19-2.02)	17.3 (14.3-21.0)	11.2	4E-10	5.53 (4.52-6.77)	13.7 (10.8-17.4)	2.47	3E-05	3.57	0.79	0.22
Gbp4		86.1 (73.9-100)	795 (523-1208)	9.23	4E-08	81.5 (70.5-94.1)	153 (112-209)	1.88	2E-03	0.95	0.19	0.20
Il12		2.85 (2.19-3.71)	11.7 (7.75-17.8)	4.12	4E-05	0.30 (0.17-0.53)	0.25 (0.14-0.43)	0.82	6E-01	0.11	0.02	0.20
ERV Env		913 (661-1261)	3398 (2240-5155)	3.7	2E-04	48.1 (42.9-53.9)	33.1 (25.7-47.5)	0.69	2E-02	0.05	0.01	0.18
Irf7		43.5 (34.1-55.5)	528 (276-1010)	12.1	2E-06	145 (83.0-253)	296 (186-469)	2.04	7E-02	3.33	0.56	0.17
Fos		16.6 (11.9-23.2)	17.3 (9.38-31.8)	1.04	9E-01	20.2 (14.5-28.0)	2.39 (1.61-3.55)	0.12	5E-07	1.21	0.14	0.11
Ifih1/Mda5		8.39 (6.56-10.7)	181 (82.4-395)	21.5	2E-06	43.3 (35.5-52.8)	92.1 (75.8-112)	2.13	6E-05	5.16	0.51	0.10
Cxcl10		0.35 (0.21-0.59)	231 (81.4-655)	659	1E-08	0.26 (0.12-0.59)	16.2 (5.83-44.9)	61.7	1E-05	0.75	0.07	0.094
Mpo		0.33 (0.19-0.57)	19.5 (8.56-44.6)	59.9	6E-07	1.73 (0.71-4.26)	7.91 (2.61-24.0)	4.56	5E-02	5.32	0.41	0.076
Myc		22.4 (18.0-27.7)	294 (209-413)	13.1	3E-09	41.6 (35.9-48.3)	41.4 (25.2-68.1)	1.00	1E+00	1.86	0.14	0.076
Ngp		7.82 (4.03-15.2)	1071 (580-1977)	137	1E-08	130 (77.8-216)	1275 (1022-1589)	9.83	5E-07	16.6	1.19	0.072
Ifit1		10.7 (8.18-13.9)	309 (96.6-991)	29.0	5E-05	53.1 (32.8-85.8)	96.7 (59.0-158)	1.82	1E-01	4.98	0.31	0.063
Mx2		6.29 (5.53-7.16)	270 (158-460)	42.9	1E-09	198 (121-323)	476 (300-757)	2.41	2E-02	31.5	1.76	0.056
Cd69		14.1 (11.5-17.3)	203 (155-266)	14.4	1E-10	39.3 (34.6-44.6)	31.1 (17.3-55.9)	0.79	5E-01	2.78	0.15	0.055
Ccl4		1.84 (1.10-3.09)	217 (126-376)	118	3E-09	117 (75.4-181)	740 (487-1126)	6.33	2E-05	63.5	3.40	0.054
Gzmb		14.7 (9.75-22.1)	1063 (603-1873)	72.4	3E-09	28.8 (15.8-52.6)	103 (56.2-188)	3.57	1E-02	1.96	0.10	0.049
Tnfrsf9/Cd137		0.64 (0.46-0.89)	97.5 (47.3-201)	152	3E-09	0.76 (0.42-1.40)	3.10 (1.62-5.95)	4.06	7E-03	1.19	0.03	0.027
Cd14		44.5 (25.5-77.7)	667 (408-1091)	15.0	2E-06	88.5 (75.5-104)	19.9 (10.4-38.3)	0.23	5E-04	1.99	0.03	0.015
Nos2		0.13 (0.10-0.17)	58.9 (22.1-157)	459	4E-09	0.04 (0.03-0.05)	0.25 (0.09-0.69)	6.16	3E-03	0.31	0.00	0.013
Ifng		0.58 (0.33-1.02)	438 (178-1080)	751	3E-09	0.15 (0.08-0.29)	0.51 (0.14-1.89)	3.30	1E-01	0.26	0.00	0.004

* Gene: Mus musculus reference genome GenBank name/other name in literature. The list includes the 113 coding sequences listed in Methods and two endogenous retrovius (ERV) proteins, Env and Gag-pol.
† Heatmap (red-white-blue scale) of log-transformed "Peromyscus v Mus LPS/control" values (last column). This is ratio of "Peromyscus v Mus LPS FC" (2nd column from right) to "Peromyscus v Mus control FC" (3rd column from right)
‡ Mean unique reads for given gene normalized for reads for Ptprc (Cd45) gene for a sample. The 95% confidence intervals (CI) are asymmetric. Actual [gene]/Ptprc ratios are X 10^-3.
** Other abbreviations: Peromyscus, Peromyscus leucopus; Mus, Mus musculus FC, fold-change; FDR, false discovery rate

To assess differences by sex among *P. leucopus* in their responses to LPS, we used the original reads from 20 deermice from the previous blood RNA-seq study in combination with the data for 20 deermice of the present study for the targeted RNA-seq. This yielded 11 deermice of each sex receiving LPS in the same dose and 9 animals of each sex receiving saline instead. Using *Z*-scores to provide comparability across studies and after correcting for multiple testing, we found no difference between females and males in their responses, beyond a tendency for Il6 and Il10 expression to be higher in males than females in the LPS treatment group.

"Alternatively-activated" macrophages and "nonclassical" monocytes in *P. leucopus*

While we could not type single cells using protein markers, we could assess relative transcription of established indicators of different white cell subpopulations in whole blood. The present study, which incorporated outbred *M. musculus* instead of an inbred strain, confirmed the previous finding of an inversion between Nos2 and Arg1 expression: that is, high Nos2 and low Arg1 in *M. musculus* and the opposite in *P. leucopus* (Figure 4; Table 2). The RNA-seq findings were confirmed by specific RT-qPCR assays for Nos2 and Arg1 transcripts for *P. musculus* and *M. musculus* (Table 3).

Table 3. RT-qPCR of blood of LPS-treated *P. leucopus* and *M. musculus*

Blood mRNA source	Control mean copies (95% CI)	LPS mean copies (95% CI)	Fold difference LPS/control	*t* test *p* value/Mann-Whitney *p* value
P. leucopus				
Gapdh	1.22 (0.40-3.74) x 10^5	2.38 (1.10-5.16) x 10^5	1.95	0.35/0.49
Nos2	191 (141-260)	138 (61-315)	0.72	0.47/0.53
Arg1	4.62 (3.09-6.92) x 10^3	12.3 (3.22-47.1) x 10^3	2.66	0.18/0.55
M. musculus				
Gapdh	6.10 (2.32-16.0) X 10^6	1.77 (0.80-3.89) X 10^6	0.29	0.06/0.02
Nos2	101 (68-151)	1891 (866-4130)	18.6	<0.00001/0.002
Arg1	27 (15-20)	16 (8-34)	0.59	0.29/0.45

Low transcription of Nos2 and high transcription of Arg1 both in controls and LPS-treated *P. leucopus* was also observed in the experiment where the dose of LPS was 1 μg/g body mass instead of 10 μg/g and the interval between injection and assessment was 12 h instead of 4 h (Table 4). We previously showed that the Nos2-Arg1 relationship in deermice was not limited to response to LPS; *P. leucopus* that were bacteremic with the relapsing fever agent *Borrelia hermsii* had no detectable transcripts for Nos2 but a higher amount of transcription of Arg1 in the blood in comparison to uninfected animals (Balderrama-Gutierrez et al. 2021).

Table 4. Targeted RNA-seq of *P. leucopus* blood in 12 h and 1 μg/g LPS experiment

Gene	Control (n=3) mean (95% CI)*	LPS (n=3) mean (95% CI)*	Fold change	FDR *p* value†
Akt1	220 (12-4202)	514 (321-825)	2.3	0.05
Akt2	145 (97-217)	336 (236-478)	2.3	0.04
Arg1	146 (58-367)	2812 (273-28925)	19	0.018
Cd14	82 (12-569)	914 (161-5197)	11	0.05
Cd69	165 (87-310)	68 (14-329)	0.42	0.15
ERV Env	25 (3-242)	40 (7-224)	1.6	0.86
ERV Gag-pol	3085 (132-14695)	2768 (533-1278)	0.9	0.66
Fcgr3/Cd16	40 (25-66)	841 (533-1278)	21	0.008
Gapdh	7176 (3504-15142)	23811 (5827-97306)	3.3	0.07
Gbp4	97 (6-1551)	439 (33-5819)	4.5	0.05
Ifit1	367 (51-2663)	1373 (374-5047)	3.7	0.05
Ifng	0 (0-0)	0 (0-0)	.	.
Il1b	258 (18-3652)	1432 (183-11220)	5.6	0.1
Irf7	121 (93-157)	11405 (530-245616)	94	0.003
Isg15	429 (184-1001)	19505 (11140-34152)	45	0.005
Mx2	157 (73-341)	1310 (323-5315)	8.3	0.04
Nos2	0 (0-0)	0 (0-0)	.	.
Oas1	65 (31-138)	1458 (367-5795)	22	0.03
Rigi/Ddx58	38 (3-504)	173 (35-845)	4.5	0.07
Saa3	2 (0-250)	6683 (1494-29896)	3372	0.03
Slpi	6 (1-46)	779 (326-1864)	123	0.03
Sod2	180 (54-607)	3406 (698-16633)	19	0.03

* Mean unique reads for given gene normalized for reads for Ptprc (Cd45) gene for a sample. The 95% confidence intervals (CI) are asymmetric. Actual [gene]/Ptprc ratios are X 10^-3.

† FDR, false discovery rate

In addition to the ratio of Nos2 to Arg1 expression for typing macrophage and monocyte subpopulations, there are also the relative expressions of three other pairs of genes: (1) IL12 and IL10, where a lower IL12/IL10 ratio is more characteristic of alternatively activated or M2 type (van Stijn et al. 2015; P.J. Murray 2017); (2) the proto-oncogene kinases Akt1 and Akt2, where the associations are Akt1 with M2-type and Akt2 with M1-type macrophages (Vergadi et al. 2017; Arranz et al. 2012); and (3) CD14 and CD16 (low affinity immunoglobulin gamma Fc region receptor III; Fcgr3), where low expression of CD14 and high expression of CD16/Fcgr3 is associated with "non-classical" monocytes (Narasimhan et al. 2019). There is evidence that nonclassical monocytes can change to M2-type macrophages (Italiani and Boraschi 2014).

These four relationships, which are presented as log-transformed ratios of Nos2/Arg1, IL12/IL10, Akt1/Akt2, and CD14/CD16, are shown in Figure 5. The differences between *P. musculus* and *M. musculus* in the ratios of Nos2/Arg1 and IL12/IL10 were reported before (Balderrama-Gutierrez et al. 2021), and the present study with outbred mice and normalization for white cells replicated those findings. In both species the Akt1/Akt2 ratio declined in LPS-treated animals, but for *P. leucopus* the ratio remained > 1.0 even among LPS-treated animals, while in the blood of *M. musculus* the ratio was < 1.0 at baseline and declined further in the LPS-treated animals.

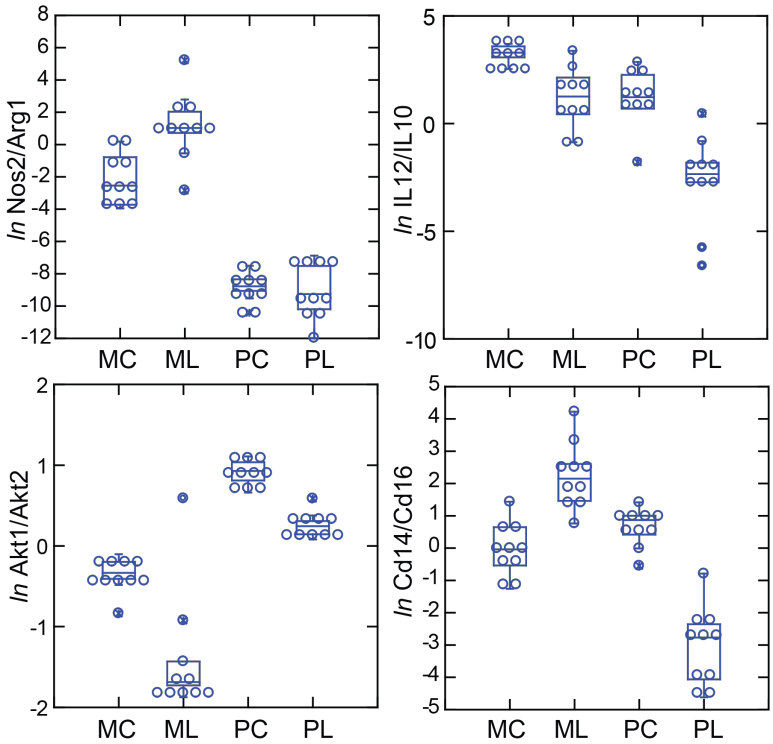

Figure 5. Box plots of log-transformed ratios of four pairs of gene transcripts from targeted RNA-seq analysis of blood of *P. leucopus* (P) or *M. musculus* (M) with (L) or without (C) treatment with LPS.

An ortholog of Ly6c (Bothwell, Pace, and LeClair 1988), a protein used for typing mouse monocytes and other white cells, has not been identified in *Peromyscus* or other Cricetidae family members, so the comparison with Cd14 is with Cd16 or Fcgr3, which cricetines like humans do have. In mice the Cd14/Cd16 ratio increased from baseline in the LPS group. In the deermice the ratio in control animals was midway between the two groups of mice but there was a marked decrease in the LPS-treated deermice (Figure 5). This was not associated with a fall in the absolute numbers or percentages of monocytes in the blood of these animals.

Taken together, the Nos2-Arg1, Il12-Il10, Akt1-Akt2, and CD14-CD16 relationships document a disposition toward alternatively-activated macrophages and nonclassical monocytes in *P. leucopus* both before and after exposure to LPS. This contrasts with profiles consistent with a predominance of classically-activated macrophages and classical monocytes in mice.

Interferon-gamma and interleukin-1 beta dichotomy between deermice and murids

For mice the Ifng transcript was one of the top ranked DEGs by both fold-change and adjusted *p* value by genome-wide RNA-seq (Table 2). In contrast, for *P. leucopus* Ifng was far down the list and the comparably ranked DEG instead was Il1b. This inversion of relationships between two pro-inflammatory cytokines was confirmed by analysis of the individual animals of both species (Figures 6). There was little or no detectable transcription of Ifng in the blood of deermice in which Il1b expression was high. There was also scant to no transcription of Ifng in the blood of *P. leucopus* 12 h after injection of LPS (Table 4).

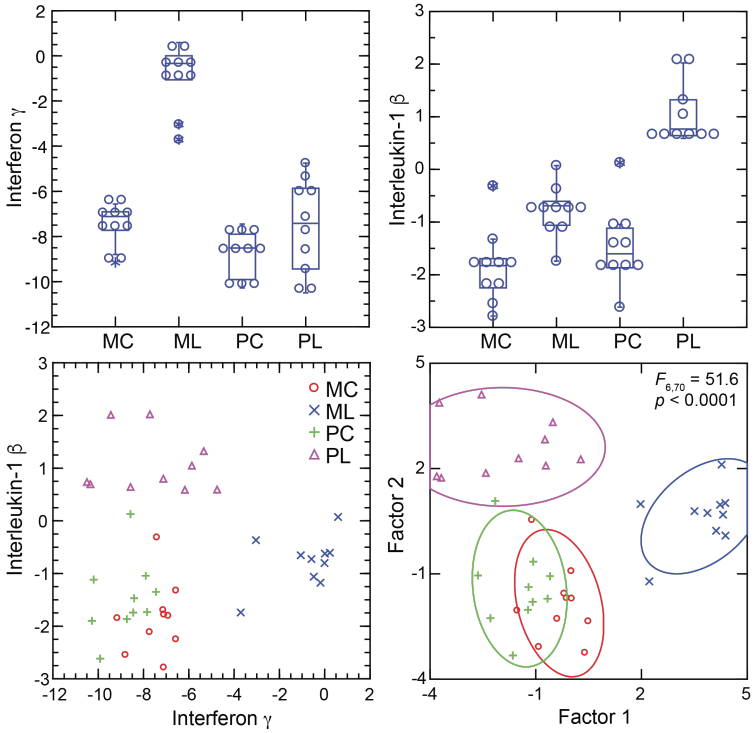

Figure 6. Transcripts of interferon-gamma (γ) and interleukin-1 beta (β) by targeted RNA-seq of the blood of *P. leucopus* (P) or *M. musculus* (M) with (L) or without (C) treatment with LPS. The top panels are box plots of the individual values. The lower left panel is a scatter plot of interleukin-1 β on interferon- γ values. The lower right panel is a Discriminant Analysis of these pairs of values where Factor 1 corresponds to interferon- γ, and Factor 2 corresponds to interleukin-1 β.

The up-regulation of Ifng within 4 hours of exposure to LPS was not limited to the species *M. musculus*. In an experiment with the rat *R. norvegicus*, we used two different LPS doses (5 μg/g and 20 μg/g) but the same 4 h endpoint and whole blood as the sample. Both groups of LPS-treated rats had lowered total white blood cells and, like the mice, lower neutrophil-to-lymphocyte ratios compared to controls (Table 5). There were also marked elevations of interferon-gamma, interleukin-6 and interleukin-10 proteins from undetectable levels in the blood of the treated rats. By targeted RNA-seq there were 24x fold-changes between the LPS-treated rats and control rats for Ifng and Nos2 but only ~3x fold-change for Il1b. We also noted that in the rat the Nos2-Arg1, Il12-Il10, Akt1-Akt2, and CD14-CD16 relationships that serve to signify monocyte and macrophage phenotypes resembled those of the mice and not what was observed in deermice.

Table 5. Hematology, cytokines, and targeted RNA-seq of LPS-treated and control rats

Variable	Control (n=5) mean (95% CI)*	LPS (n=11) mean (95% CI)*,†	Fold change	FDR *p* value
Hematology				
Hematocrit (%)	48 (46-50)	48 (46-49)	1.0	1E+00
White blood cells	7660 (7200-8310)	4980 (2020-7940)	0.75	2E-01
Neutrophils	3680 (3260-4090)	1410 (520-2290)	0.38	4E-03
Lymphocytes	3170 (3010-3330)	2830 (1230-4430)	0.89	8E-01
Neutrophil/lymphocyte	1.17 (1.01-1.33)	0.49 (0.44-0.55)	0.42	7E-09
Plasma cytokines (pg/ml)				
Interleukin-6	0 (0-0)	36933 (21676-52190)	.	5E-15
Interleukin-10	9 (1-17)	640 (477-802)	71	2E-09
Interferon-gamma	0 (0-0)	9091 (7126-11056)	.	9E-20
Targeted RNA-seq				
Akt1	35.8 (29.8-42.9)	24.3 (21.5-27.5)	0.68	4E-03
Akt2	50.8 (44.9-57.4)	109 (95.2-125)	2.2	9E-06
Arg1	0.04 (0.02-0.08)	0.21 (0.10-0.44)	4.8	2E-02
Cd14	7.7 (5.3-11.2)	43.4 (29.6-63.6)	5.6	9E-05
Cd177	0.89 (0.43-1.8)	190 (143-251)	213	2E-10
Cd3	32.3 (27.7-37.6)	21.9 (18.5-25.8)	0.68	1E-02
Cd69	17.9 (16.7-19.2)	58.9 (49.1-70.7)	3.3	9E-07
Cgas	1.5 (1.3-1.6)	12.8 (10.8-15.1)	8.7	3E-10
Cxcl10	0.43 (0.34-0.56)	130 (93.7-181)	302	1E-11
Dhx58	7.1 (6.7-7.6)	113 (97.3-130)	15.8	3E-12
ERV Env	8.4 (7.5-9.3)	713 (624-815)	85.3	1E-14
ERV gag-pol	6.0 (5.4-6.7)	506 (449-570)	84.3	7E-15
Fcgr2a	114 (87.0-150)	764 (631-925)	6.7	4E-08
Fcgr2b	32.5 (24.6-43.1)	161 (127-204)	4.9	2E-06
Fcgr3/Cd16	15.2 (13.6-17.0)	13.9 (11.8-16.3)	0.91	5E-01
Gapdh	327 (237-451)	1643 (1385-1949)	5.0	2E-07
Gbp4	35.7 (33.6-38.0)	269 (237-306)	7.5	3E-11
Ibsp	0.41 (0.31-0.55)	0.61 (0.47-0.80)	1.5	1E-01
Ifih1	18.7 (17.1-20.4)	165 (149-184)	8.8	2E-12
Ifit1	102 (70.0-147)	756 (677-844)	7.4	3E-09
Ifng	0.47 (0.32-0.67)	10.3 (6.4-16.5)	22.1	1E-06
Il10	0.12 (0.07-0.21)	4.5 (3.4-5.8)	38.2	5E-09
Il12	0.07 (0.04-0.11)	3.2 (2.0-4.9)	45.9	7E-08
Il1b	58.6 (39.7-86.4)	618 (503-760)	10.6	2E-08
Il6	0.06 (0.05-0.08)	4.4 (2.9-6.6)	70.9	6E-09
Irf7	44.8 (36.9-54.3)	443 (372-528)	9.9	6E-10
Isg15	15.6 (13.1-18.7)	624 (534-729)	39.9	6E-13
Itgam?Cd11b	66.3 (52.5-83.7)	208 (161-269)	3.1	9E-05
Mmp8	75.2 (50.4-112)	519 (438-615)	6.9	7E-08
Mx2	40.7 (35.9-46.2)	900 (780-1039)	22.1	1E-12
Nos2	32.4 (17-60.6)	2990 (2491-3589)	92.4	1E-10
Oas1	23.1 (18.8-28.4)	151 (140-164)	6.6	3E-11
Rigi/Ddx58	8.6 (7.8-9.4)	151 (135-168)	17.6	1E-13
S100a9	298 (190-466)	2884 (2269-3666)	9.7	2E-07
Saa1	0.60 (0.49-0.73)	699 (552-884)	1167	4E-14
Slpi	20.2 (13.1-31.3)	262 (197-347)	12.9	1E-07
Sod2	63.8 (51.1-79.6)	901 (759-1070)	14.1	2E-10
Tlr4	5.3 (4.6-6.0)	20.1 (17.2-23.6)	3.8	8E-08
Tnf	1.1 (0.63-1.9)	78.8 (62.6-99.1)	72.8	2E-10
Ratios				
Akt1/Akt2	0.70 (0.65-0.76)	0.22 (0.19-0.25)	0.31	2E-08
Cd14/Fcgr3	0.51 (0.34-0.76)	3.14 (2.26-4.36)	6.16	1E-05
IL12/IL10	0.54 (0.22-1.37)	0.70 (0.51-0.95)	1.30	5E-01
Nos2/Arg1	741 (403-1362)	14244 (7615-26646)	19.2	5E-05

* For targeted RNA-seq it is mean unique reads for given gene normalized for reads for Ptprc (Cd45) gene for a sample. The 95% confidence intervals (CI) are asymmetric. Actual [gene]/Ptprc ratios are X

† The results for rats receiving 5 μg/g (n=6) and 20 μg/g (n=5) were combined

We asked why the interferon-gamma response observed in CD-1 mice and rats here was not as pronounced in BALB/c mice (Balderrama-Gutierrez et al. 2021). Accordingly, we used the RNA-seq reads from the prior study in combination with the reads of the present study and carried out targeted RNA-seq as described (Supplementary Materials Figure S1). The BALB/c inbred mice had, like the CD-1 mice, modest elevations of Il1b transcription. Ifng expression was also elevated in the BALB/c animals but not to the degree noted in CD-1 mice or rats. An explanation for this may be an inherent difference of BALB/c mice from other strains in their lower interferon-gamma response to LPS (Soudi et al. 2013; Kuroda, Kito, and Yamashita 2002).

Interferon-gamma and inducible nitric oxide synthase

Interferon-gamma is a determinant of Nos2 expression (Lowenstein et al. 1993; Salkowski et al. 1997). So, the scant transcription of Ifng in *P. leucopus* conceivably accounted for the low expression of Nos2 in that species, not only with LPS but also during bacterial infection. The analysis shown in upper

left panel of Figure 7 shows a tight correlation between the levels of transcription of Ifng and Nos2 for both species and both experimental conditions. A significant correlation was also observed for the combined set of animals between the ratios of Nos2 to Arg1 and Ifng to Il1b (upper right panel), an indication of co-variation between Ifng expression and macrophage polarization.

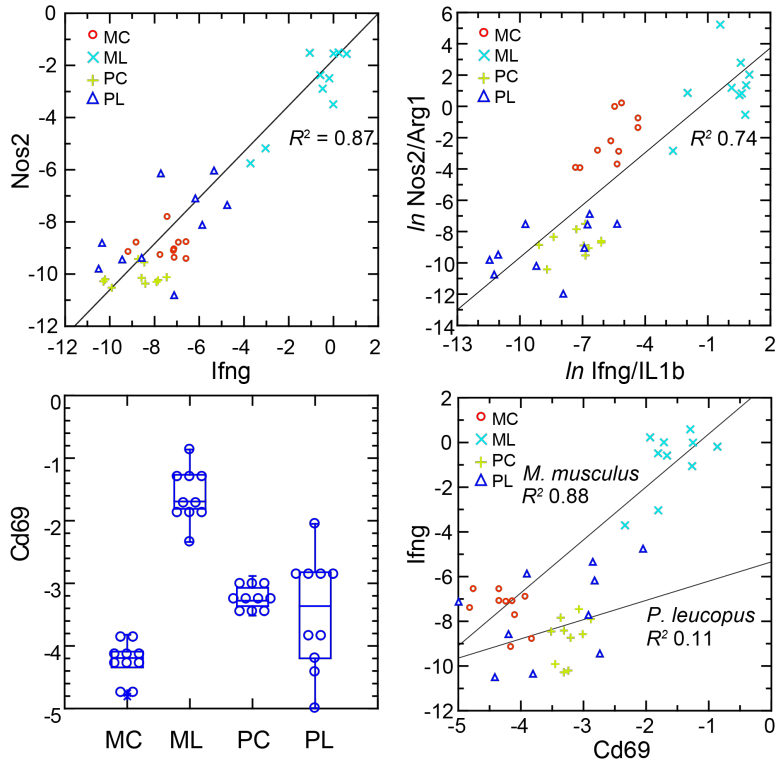

Figure 7. Normalized transcripts of Nos2, Ifng, and Cd69 in targeted RNA-seq analysis of blood of *P. leucopus* (P) or *M. musculus* (M) with (L) or without (C) treatment with LPS. Upper left: scatter plot of individual values for Nos2 on Ifng with linear regression curve and coefficient of determination (R^2). Upper right: natural logarithm (*ln*) of ratios of Nos2/Argi1 on Ifng/IL1b with regression curve and R^2. Lower left: Box plots of individual values of normalized transcripts of Cd69. Lower right: Scatter plot of Ifng on Cd69 with separate regression curves and R^2 values for *M. musculus* and *P. leucopus*.

The plausible sources of Ifng mRNA in whole blood are T-cells, Natural Killer (NK) cells, and Type 1 Innate Lymphoid Cells (ILC1) (Quatrini et al. 2017). A DEG for *M. musculus* by both genome-wide and targeted RNA-seq (Table 2; Table S2) was Cd69, a C-type lectin protein and an early activation antigen for these cells (Heinzelmann et al. 2000). In *P. leucopus* transcription Cd69 occurred in the blood of control *P. leucopus* but it was the same or only marginally different for the LPS-treated animals (lower left of Figure 7). In contrast, in *M. musculus* the baseline transcription of Cd69 was below that of *P. leucopus*, but in the LPS-treated mice it was many fold higher. In mice transcripts for Cd69 correlated tightly with Ifng transcription, while in the deermice there was little correlation between Cd69 and Ifng expression at those low levels (lower right).

The findings are consistent with CD69-positive cells being a source of Ifng in mice. Cd69 transcription was comparatively higher in control deermice than in control mice, so we presume that deermice have CD69-positive cells at baseline. One explanation then for the comparatively few Ifng transcripts in the deermice after LPS is a diminished responsiveness of these cells. Tlr4 expression increased ~3 -fold more in *P. leucopus* than in *M. musculus* after LPS, but the magnitude of the relative decline in expression of Cd14 in deermice than mice was even greater (Table 2). CD14 is required for the LPS-stimulated signaling through surface TLR4 (Mazgaeen and Gurung 2020), and, as such, its decreased availability for this signaling pathway is a possible explanation for the moderated response to LPS in *P. leucopus*.

Interferon-stimulated genes and RIG-I-like receptors

As noted, GO terms differentiating mice from deermice included "response to interferon-beta" and "response to virus" (Figure 3). There was also the example of Mx2, an ISG with anti-viral activity on its own, that showed a greater fold-change from baseline in mice than in deermice (Figure 4 and Table 2). Five other ISGs--guanylate binding protein 4 (Gbp4), interferon-induced protein with tetratricopeptide repeat (Ifit1), interferon regulatory factor 7 (Irf7), ubiquitin-type modifier ISG15 (Isg15), and 2′-5′ oligoadenylate synthase 1A (Oas1a)—had elevated transcription in all LPS-treated animals. But the magnitude of fold change was less in the deermice, ranging from 6-25% of what it was in the LPS group of mice (Table 2).

The up-regulation of these ISGs was evidence of type 1 interferon action, but transcripts for interferon-1 beta (Ifnb) or -alpha (Ifna) themselves were scarcely detectable in deermice or mice in the blood under either condition. We then considered pattern recognition receptors (PRR) that conceivably part of a signaling pathway leading to ISG expression. Among the DEGs from the genome-wide analyses were four cytoplasmic PRRs (Table S2): (1) Rigi (formerly Ddx58), which encodes the RNA helicase retinoic acid-inducible I (RIG-I); (2) Ifih1, which encodes interferon induced with helicase C domain 1, also known as MDA5 and a RIG-I-like receptor; (3) Dhx58, also known LGP2 and another RIG-I-like receptor; and (4) cGAS (cyclic GMP-AMP synthase), which is part of the cGAS-STING sensing pathway.

	Cgas	Dhx58	Ifih1	Rigi	Gbp4	Irf7	Isg15	Mx2	Oas1
Cgas	1.00	0.70	0.78	0.40	0.46	0.63	0.39	0.77	0.61
Dhx58		1.00	0.86	0.80	0.76	0.79	0.61	0.58	0.62
Ifih1			1.00	0.54	0.59	0.79	0.61	0.77	0.75
Rigi				1.00	0.83	0.52	0.43	0.20	0.26
Gbp4					1.00	0.52	0.43	0.24	0.24
Irf7						1.00	0.81	0.71	0.77
Isg15							1.00	0.48	0.59
Mx2								1.00	0.87
Oas1									1.00

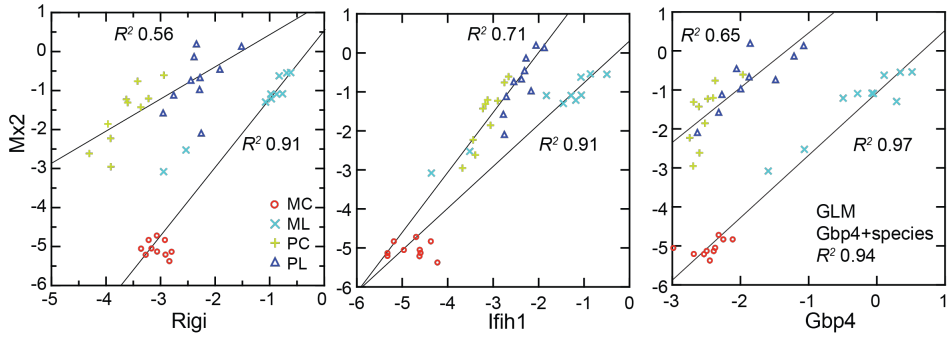

Figure 8. Co-variation between transcripts for selected PRRs (yellow) and ISGs (gree) in the blood of *P. leucopus* (P) or (M) with (L) or without (C). Top panel: matrix of coefficients of determination (R^2). Bottom panels: scatter plots of log-transformed normalized Mx2 transcripts on Rigi (left), Ifih1 (center), and Gbp4 (right). The linear regression curves are for each species. For the right bottom graph the results from the General Linear Model (GLM) estimate are given.

All four of these cytoplasmic PRRs were up-regulated in blood of LPS-treated mice and deermice (Table 2). But, again, for each of them the magnitude of fold change was less by 50-90% in treated *P. leucopus* than in *M. musculus*. The coefficients of determination for the 6 ISGs and the 4 PRRs are provided in Figure 8. For most of the pairs there was evidence of covariation across all 40 animals. When the correlation was low across all the data, e.g. between the ISG Mx2 and the PRR Rigi or the ISGs Mx2 and Gbp4, it was high within a species.

These findings were evidence that pathways in *P. leucopus* from PRR signaling and ISG expression functioned similarly to those in *M. musculus* but differed under these experimental conditions in magnitude of the changes, being more moderate in the deermice.

Endogenous retroviruses in deermice, mice, and rats after LPS exposure

The six ISGs are nonexclusive consequences of activity of type I interferons. What we could document was the association of transcription of the gene for the cytoplasmic PPRs, including RIG-I,

and the ISGs in both species, as well as the distinction between deermice in the magnitude of the responses of both PRRs and ISGs. These findings led us to ask what could be a pathogen-associated molecular pattern (PAMP) for signaling pathways leading to expression of type 1 interferons.

One of these is endogenous retroviruses (ERV). The activity of these diverse, abundant, and pervasive elements have been recognized as one of the drivers of innate immune responses to a microbe (Hurst and Magiorkinis 2015; Lima-Junior et al. 2021; Rangel et al. 2022). Our attention was drawn to ERVs by finding in the genome-wide RNA-seq of LPS-treated and control rats that 2 of the 3 highest scoring DEGs by FDR *p* value and fold-change were a *gag-pol* polyprotein of a leukemia virus with 131x fold-change from controls and a mouse leukemia virus (MLV) envelope (Env) protein with 62x fold-change (Table 5).

We returned to the mouse and deermouse data. There were four MLV or other ERV Env proteins among the 1266 genome-wide RNA-seq DEGs for *M. musculus*. But, there was no ERV Env protein identified as such among the 1154 DEGs identified for *P. leucopus* (Table S1; Dryad Table D1). One possible explanation for the difference was an incomplete annotation of the *P. leucopus* genome. We took three approaches to rectify this. The first was to examine the DEGs for *P. leucopus* that encoded a polypeptide ≥ 200 amino acids and was annotated for the genome as "uncharacterized". A search with these candidates of both the virus and rodent proteins databases identified two that were homologous with *gag-pol* polyproteins of ERVs, mainly leukemia viruses, of mammals.

For a second approach we carried out a de novo transcript assembly of mRNA reads from blood of LPS-treated and control *P. leucopus* and used the resultant contigs as the reference set for RNA-seq analysis. This identified two contigs that were measurably transcribed in the blood, differentially expressed between conditions, and were homologous to ERV sequences. One was revealed to be an Env protein that was identical to a *P. leucopus* protein annotated as "MLV-related proviral Env protein" (XP_037065362). The second was a *gag-pol* protein. The latter was near-identical to the *gag-pol* protein identified by the first approach.

The third approach was to scan the *P. leucopus* genome for nonredundant sequences, defined as < 95% identity, that were homologous with ERV *pol* sequences, which are not typically annotated because of masking for repetitive sequences This analysis yielded 615 unique sequences. These were used in turn as reference set for RNA-seq. There were 4 sequences that met the criterion of FDR *p* value <0.05. Three were transcribed at 5- to 40-fold higher levels in LPS-treated deermice than in controls. But all three, as well as the fourth, a down-regulated DEG, were ERV relics with truncations, frame shifts, and in-frame stop codons. These were assessed as non-coding RNAs and not further pursued in this study.

To represent *P. leucopus* in a targeted RNA-seq comparison with mice and rats we settled on the Env protein and *gag-pol* coding sequences identified present in the blood mRNA and as DEGs. Representing *M. musculus* were highest ranked MLV Env and *gag-pol* protein sequences among the DEGs. For rats we chose Env and *gag-pol* proteins that were second and third ranked DEGs identified in the genome-wide RNA-seq (Dryad table). Because of length differences for the coding sequences, the unit used for cross-species analysis was reads per kilobase before normalization for Ptprc transcription.

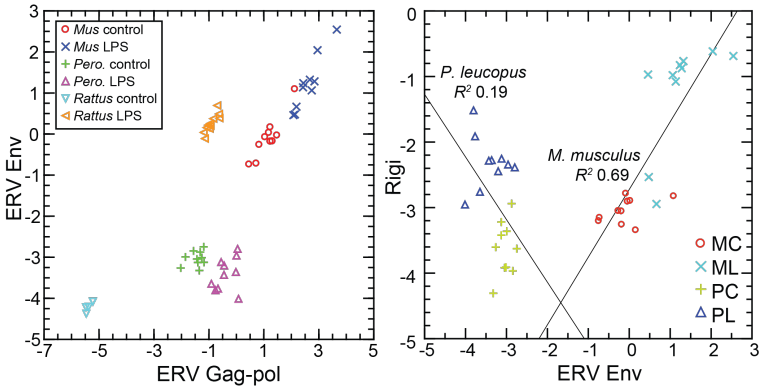

Figure 9. Scatter plots of endogenous retrovirus (ERV) Env and Gag-pol protein gene transcription (left) and association of ERV Env with Rigi transcription (right) in the blood of *P. leucopus* (*Pero*; P), *M. musculus* (*Mus*; M), or *R. norvegicus* (*Rattus*) with (L) or without (control; C) treatment with LPS. In right panel the linear regression curve and coefficients of determination (R^2) for *P. leucopus* and *M. musculus* are shown.

The left panel of Figure 9 shows the striking transcriptional fold-change in LPS-treated rats of both Env and *gag-pol* sequences over controls. Of lesser magnitude but no less significant was the fold-change observed *M. musculus* for both Env and *gag-pol* sequences. In both mice and rats Env and *gag-pol* read values were highly correlated across conditions. In contrast, in *P. leucopus* the magnitudes of fold-change upwards for *gag-pol* was less than in mice or rats, and transcription of the Env protein sequence was actually lower in LPS-treated animals than in controls. While there was a tight association between Env protein and the PRR Rigi transcription in the M. musculus, this was not observed in *P. leucopus*. Rigi transcription was moderately higher at the time that Env protein's transcription was lower in the LPS group (right panel of Figure 9).

DISCUSSION

Study limitations

The approach was forward and unbiased, looking for differences between species broadly across their transcriptomes. The findings lead to hypotheses, but reverse genetics in service of that testing was not applied here. In selective cases we could point to supporting evidence in the literature on *M. musculus* and the phenotypes of relevant gene knockouts, but there are no such resources for *Peromyscus* as yet. The resource constraint also applies to the availability of antibodies for use with *Peromyscus* for immunoassays for specific proteins, e.g. interferon-gamma, in serum, or for cell markers, e.g. CD69, for flow cytometry of white blood cells.

While a strength of the study was use of an outbred population of *M. musculus* to approximate the genetic diversity of the *P. leucopus* in the study, this meant that some genes of potential relevance might have gone undetected, i.e. from type II error. The variances for a sample of genetically diverse outbred animals, like the LL stock of *P. leucopus* (A. Long et al. 2019; P. Long et al. 2022), would be expected to be greater than for the same sized sample of inbred animals. For some traits, especially ones that are complex or under balancing selection, even sample sizes of 10 in each group may not have provided sufficient power for discrimination between deermice and mice.

The parameters for the experiment of LPS dose, the route, and duration of experiment each might have had different values under another design. Those particular choices were based on past studies of deermice and mice (Langeroudi et al. 2014; Balderrama-Gutierrez et al. 2021). In another experiment we found that with doses twice or half those given the deermice the responses by rats to the different doses were indistinguishable by hematology, cytokine assays, and RNA-seq. Thus, there seems to be some latitude in the dose and still achieving replication. We obtained similar results for *P. leucopus* when we looked at a replicate of the experiment with the same conditions (Balderrama-Gutierrez et al. 2021), when the dose was lower and duration lengthened to 12 h (this study), and when the inflammatory stimulus was bacteremia (Barbour et al. 2019). The bacterial infection experiment indicated that the observed effect in *P. leucopus* was not limited to a TLR4 agonist; the lipoproteins of *B. hermsii* are agonists for TLR2 (Salazar et al. 2009).

While the rodents in these experiments were housed in the same facility and ate the same diet, we cannot exclude inherent differences in gastrointestinal microbiota between species and individual outbred animals as co-variables for the experimental outcomes. We reported differences between the LL stock *P. leucopus* and BALB/c *M. musculus* of the same age and diet in their microbiomes by metagenomic analysis and microbiologic means (Milovic et al. 2020). This included a commensal *Tritrichomonas* sp. in *P. leucopus* but not in the *M. musculus* in the study. The presence of these protozoa affects innate and adaptive immune responses in the gastrointestinal tract (Escalante et al. 2016; Chiaranunt et al. 2022), but it is not clear whether there are systemic consequences of colonization by this flagellate.

LPS, ERVs, and interferons

The results confirm previous reports of heightened transcription of ERV sequences in mice or mouse cells after exposure to LPS (Hara et al. 1981; Jongstra and Moroni 1981; Stoye and Moroni 1983). Here we add the example of the rat. The LPS was administered in solution and not by means of membrane vesicles. The sensing PRR presumably was surface-displayed, membrane-anchored TLR4 (Mazgaeen and Gurung 2020). It follows that a second, indirect effect of LPS on the mouse is through its provocation of increased ERV transcription intracellularly. ERV-origin RNA, cDNA and/or protein would then be recognized by a cytoplasmic PRR. RIG-I was one associated with ERV transcription in this study. Kong et al. reported that LPS stimulated expression of Rigi in a mouse macrophages but did not investigate ERVs for an intermediary function in this phenomenon (Kong et al. 2009). As was demonstrated for LINE type retrotransposons in human fibroblasts, intracellular PRR signaling can trigger a type 1 interferon response (De Cecco et al. 2019). The combination of these two signaling events, i.e. one through surface TLR4 by LPS itself and another through intracellular PPR(s) by to-be-defined ERV products, manifested in mice and rats as a response profile that had features of both a response to a virus with type 1 interferon and ISGs and a response to a bacterial PAMP like LPS with acute phase reactants such as calprotectin and serum amyloid.

This or a similar phenomenon has been observed under other circumstances. In humans there was heightened transcription of retrotransposons in patients with septic shock (Mommert et al. 2020), as well as in peripheral blood mononuclear cells from human subjects experimentally injected with LPS (Pisano et al. 2020). Bacteria like *Staphylococcus epidermidis* that express TLR2 agonists, such as lipoteichoic acid, promoted expression of ERVs, which in turn modulated host immune responses (Lima-Junior et al. 2021). A synthetic analog of a *B. burgdorferi* lipoprotein activated human monocytic cells and promoted replication of the latent HIV virus in cells that were persistently infected (Norgard et al. 1996).

P. leucopus does not fit with this model. Instead of the prominent interferon-gamma response observed in mice and rats, there were prominent responses of interleukin-1 beta and genes associated with neutrophil activation. Instead of the much heightened expression of ISGs, like Mx2 and Isg15, in mice treated with LPS, the deermice under the same condition had a more subdued ISG transcription profile. Instead of increased expression of ERV Env protein sequences in blood of mice and rats treated with LPS, there was decreased transcription of the homologous MLV Env gene in like-treated *P. leucopus*.

Our first annotation of the *P. leucopus* genome did not identify the gene for zinc finger protein 809 (Zfp809) (A. Long et al. 2019), a KRAB domain protein that initiates ERV silencing (Wolf et al. 2015). But subsequent rounds of annotation confirmed genes and transcripts for Zfp809 in both *P. leucopus* (XP_028728362) and *P. maniculatus* (XP_006982432). In neither deermice nor mice nor rats was Zfp809 among the up- or down-regulated DEGs with LPS (Dryad Table D1).

Reducing the differences between *P. leucopus* and the murids *M. musculus* and *R. norvegicus* to a single all-embracing attribute may be fruitless. But from a perspective that also takes in the 2-3x longer life span of the white-footed deermouse compared to the house mouse and the capacity of *P. leucopus* to serve as disease agent reservoir while maintaining if not increasing its distribution (Moscarella et al. 2019), the feature that seems to best distinguish the deermouse from either the mouse or rat is its predominantly anti-inflammatory quality. The presentation of this trait likely has a complex, polygenic basis, with environmental (including microbiota) and epigenetic influences. An individual's placement is on a spectrum or, more likely, a landscape rather than in one or another binary or Mendelian category.

One argument against a purely anti-inflammatory characterization is the greater neutrophil numbers and activity in *P. leucopus* compared to *M. musculus* in the LPS experiment. The neutrophil activation, migration, and phagocytosis would be appropriate early defenses against a pyogenic pathogen. But if not contained, they bring local and systemic risks for the host. This damage would not likely be from nitric oxide and reactive nitrogen species, given the minimal Nos2 transcription. But deermice showed heightened expression of proteases, such as Mmp8, enzymes for reactive oxygen species, such as NADPH oxidase 1 (Nox1), and facilitators of neutrophil extracellular traps, such as

PAD4 (Padi4) (Table 2). We had previously identified possible mitigators, such as the protease inhibitor Slpi and superoxide dismutase 2 (Balderrama-Gutierrez et al. 2021). These findings were replicated here. The topic of neutrophil activation and these and other possible counters is considered in more detail elsewhere.

An anti-inflammatory disposition but at what cost?

An assignment of infection tolerance to a host and pathogen pairing assumes sufficient immunity against the microbe to keep it in check if elimination fails. *P. leucopus*, *P. maniculatus*, and likely some other *Peromyscus* species are in this sense "immunocompetent" with respect to the microbes they host and with which they may have a long history (Hoen et al. 2009). Yet, has this balance of resistance and tolerance for certain host-associated microbes been achieved in a trade-off that entails vulnerabilities to other types of agents?

The selection of LPS as the experimental model meant to cover this contingency, at least for the common denominator of acute inflammation many types of infections elicit. But LPS studies revealed potential weaknesses of *P. leucopus* that some pathogens might exploit. One of these is the low expression of inducible nitric oxide. Although Nos2 gene knockouts in *M. musculus* had lower LPS-induced mortality than their wild-type counterparts, the mutants were more susceptible to the protozoan *Leishmania major* and the facultative intracellular bacterium *Listeria monocytogenes* (Wei et al. 1995; MacMicking et al. 1995). While there are no known studies of either of these pathogens in *P. leucopus*, the related species *P. yucatanicus* is the main reservoir for *Leishmania mexicana* in Mexico (Chable-Santos et al. 1995). Compared with *M. musculus*, which suffer a high fatality rate from experimental infections with *L. mexicana*, *P. yucatanicus* infections are commonly asymptomatic (Loría-Cervera et al. 2018).

Given the restrained interferon and ISG response shown by *P. leucopus*, another plausible vulnerability would be viral infections. But other studies indicate that neither RNA nor DNA viruses pose an inordinately high risk for *Peromyscus*. Both tolerance of and resistance to the tickborne encephalitis flavivirus Powassan virus by *P. leucopus* were demonstrated in an experimental model in which mice, by contrast, were severely affected (Mlera et al. 2017). *P. maniculatus* and *P. leucopus* have been successfully infected with the SARS-CoV-2 virus by the respiratory route, but the infected animals displayed only mild pathology, manifested little if any disability, and recovered within a few days (Fagre et al. 2021; Griffin et al. 2021; Milovic et al. 2023). Among natural populations and in the laboratory *P. maniculatus* is noted for its tolerance of hantavirus, which commonly is fatal for infected humans (Childs et al. 1994; Botten et al. 2000). *P. maniculatus* was permissive of infection with monkeypox virus, but the infection was mild and transient (Deschambault et al. 2023).

Implications for Lyme disease and other zoonoses

Our studies of *P. leucopus* began with a natural population and documented a >80% prevalence of infection and high incidence of re-infections by *B. burgdorferi* in the area's white-footed deermouse, the most abundant mammal there (Bunikis et al. 2004). This was a Lyme disease endemic area (Diuk-Wasser et al. 2012), where residents frequently presented for medical care for a variety of clinical manifestations, from mild to serious, of *B. burgdorferi* infection (Steere et al. 1986). Subclinical infections in humans occur, but most of those who become infected have a definable illness (Steere et al. 1998). The localized or systemic presence of the microbe is a necessary condition for Lyme disease, but the majority of the symptoms and signs are attributable to inflammation elicited by the organism's presence and not from virulence properties per se or the hijacking of host cells (Coburn et al. 2021). Since humans are transmission dead-ends for *B. burgdorferi* and many other zoonotic agents in their life cycles, it is not surprising that human infections are generally more debilitating if not fatal than what adapted natural hosts experience.

It is in the space between the asymptomatic natural host and symptomatic inadvertent host where there may be insights with basic and translational application. With this goal, we consider the ways the results inform studies of the pathogenesis of Lyme disease, where "disease" includes lingering disorders akin to "long Covid" (Nathan 2022), and where "pathogenesis" includes both microbial and host contributions. Plausibly-germane deermouse-mouse differences identified in our studies to date are summarized in Figure 10. Two are further highlighted here.

	Mus musculus	Peromyscus leucopus
Interferon-gamma	+++	+
Interleukin-1 beta	+	+++
NO synthase 2	+++	+
Arginase 1	+	+++
Akt1/Akt2	< 1.0	> 1.0
Cd14/Cd16	> 1.0	< 1.0
Cd69	++	±
ISGs	+++	++
RIG-I, MDA5	+++	+
Env-ERV	++	-

Figure 10. Summary of distinguishing features of transcriptional responses in the blood between *P. leucopus* and *M. musculus* 4 h after treatment with LPS. There is semi-quantitative representation of relative transcription of selected coding sequences or ratios of transcription for selected pairs of genes in the blood.

The first is macrophage polarization (Murray 2017). By the criteria summarized above, the response to LPS by *P. leucopus* is consistent with the alternatively-activated or M2 type, rather than the expected classical or M1 type. But it was not only LPS-treated deermice that had this attribute, the blood of untreated animals also displayed M2 type polarization features. This included a comparatively high Arg1 expression level and a Akt1/Akt2 ratio of less than 1 at baseline in the study. This suggests that studies of other mammals, including humans, need not administer LPS or other TLR agonist to assess a blood specimen by selected RT-qPCR or equivalent assay for a disposition toward M1 or M2-type polarization. This reading could serve as a prognostic indicator of the inflammatory response to infection with *B. burgdorferi* or other pathogen and the long-term outcome.

The second difference we highlight is the activation of ERV transcription that was prominent in the LPS-treated mice and rats but not in similarly-treated deermice. A paradoxical enlistment of antiviral defenses, including type 1 and type 2 interferons, for an infection with an extracellular bacterium, like *B. burgdorferi*, may bring about more harm than benefit, especially if the resultant inflammation persists after antibiotic therapy. There are various ways to assess ERV activation in the blood, including assays for RNA, protein, and reverse transcriptase activity. A xenotropic MLV-related retrovirus has been discounted as a cause of chronic fatigue syndrome (McClure and Kaye 2010). However, production of whole virions need not occur for there to be PRR signaling in response to cytoplasmic Env protein, single stranded RNA, or cDNA (Russ and Iordanskiy 2023).

METHODS

Animals

The study was carried out in accordance with the *Guide for the Care and Use of Laboratory Animals: Eighth Edition* of the National Academy of Sciences (https://nap.nationalacademies.org/read/12910). The protocols AUP-18-020 and AUP-21-007 were approved by the Institutional Animal Care and Use Committee of the University of California Irvine.

Peromyscus leucopus, here also referred to simply as "deermice", were of the outbred LL stock, which originated with 38 animals captured near Linville, NC and thereafter comprised a closed colony without sib-sib matings at the *Peromyscus* Genetic Stock Center at the University of South Carolina (Joyner et al. 1998). The LL stock animals for this study were bred and raised at the vivarium of University of California Irvine, an AAALAC approved facility. Outbred *Mus musculus* breed CD-1, specifically Crl:CD1(ICR) IGS, and here also referred to as "mice", were obtained from Charles River. Fischer F344 strain inbred *Rattus norvegicus*, specifically F344/NHsd, and here also referred to as "rats", were obtained from Charles River.

For the combined *P. leucopus-M. musculus* experiment the 20 *P. leucopus* were of a mean (95% confidence interval) 158 (156-159) days of age and had a mean 21 (19-22) g body mass. The 20 *M. musculus* were all 149 days of age and had a mean body mass of 47 (43-50) g. The ratio of average male to average female body mass was 1.04 for *P. leucopus* and 1.03 for *M. musculus*. The 6 female *P. leucopus* for the 12 h duration experiment were of a mean 401 (266-535) days of age and had mean body mass of 20 (17-23) g. The 16 adult 10-12 week old female *R. norvegicus* had a mean 139 (137-141) g body mass.

Animals were housed in Techniplast-ventilated cages in vivarium rooms with a 16 h-8 h light-dark cycle, an ambient temperature of 22 °C, and on ad libitum water and a diet of 2020X Teklad global soy protein-free extruded rodent chow with 6% fat content (Envigo, Placentia, CA).

For injections the rodents with anesthetized with inhaled isoflurane. The rodents were euthanized by carbon dioxide overdose and intracardiac exsanguination at the termination of the experiment. No animals died or became moribund before the 4 hour or 12 h termination time points.

LPS experiments

P. leucopus and *M. musculus* combined experiment. All treatments were administered in the morning of a single day. At 15 min intervals and alternating between species, sex, and treatments, animals were intraperitoneally (ip) injected 50 μl volumes of either ion-exchange chromatography purified *Escherichia coli* O111:B4 LPS (Sigma-Aldrich L3024, batch 0000109071; <1% protein and <1% RNA) in a dose of 10 μg per g body mass or the diluent alone: sterile-filtered, endotoxin-tested 0.9% sodium chloride (Sigma-Aldrich S8776). The animals were visually monitored in separate cages continuously for the duration of the experiment. We recorded whether there was reduced activity by criterion of huddling with little or movement for > 5 min, ruffled fur or piloerection), or rapid respiration rate or tachypnea. At 4.0 h time after injection animals were euthanized as described above, and sterile dissection was carried out immediately.

Lower dose and longer duration experiment. In an experiment with 6 *P. leucopus*, the animals were administered the same single dose of LPS but at 1.0 μg/g and the same control solution. The animals were euthanized 12 h after the injection the following day.

Rat LPS experiment. The same experimental design was used for the rats as for the combined deermice-mice experiment, with the exception that the formulation of the *E. coli* O111:B4 LPS was "cell culture grade" (Sigma-Aldrich L4391), and the groups were sterile saline alone (n = 5), 5 μg LPS per g body mass (n = 6), or 20 μg LPS per g (n = 5).

Hematology and plasma analyte assays

For the combined *P. leucopus-M. musculus* experiment automated complete blood counts with differentials were performed at Antech Diagnostics, Fountain Valley, CA on a Siemens ADVIA 2120i with Autoslide hematology instrument with manual review of blood smears by a veterinary pathologist. For the 12 h duration *P. leucopus* experiment hematologic parameters were analyzed on an ABCVet Hemalyzer automated cell counter instrument at U.C. Irvine. For the rat experiment complete blood counts with differentials were performed at the Comparative Pathology Laboratory of the University of California Davis. Multiplex bead-based cytokine protein assay of the plasma of the rats was performed at Charles River Laboratories using selected options of the Millipore MILLIPLEX MAP rat cytokine/chemokine panel.

RNA extraction of blood

After the chest cavity was exposed, cardiac puncture was performed through a 25 gauge needle into a sterile 1 ml polypropylene syringe. After the needle was removed, the blood was expelled into Becton-Dickinson K2E Microtainer Tubes, which contained potassium EDTA. Anticoagulated blood was split into a sample that was placed on ice for same-day delivery to the veterinary hematology laboratory and a sample intended for RNA extraction which was transferred to an Invitrogen RiboPure tube with DNA/RNA Later and this suspension was stored at -20 °C. RNA was isolated using the Invitrogen Mouse RiboPure-Blood RNA Isolation Kit]. RNA concentration was determined on a NanoDrop microvolume spectrophotometer (ThermoFisher) and quality was assessed on an Agilent Bioanalyzer 2100.

RNA-seq

For the *P. leucopus*, *M. musculus*, and *R. norvegicus* RNA extracts of whole blood production of cDNA libraries was with the Ilumina TruSeq Stranded mRNA kit. After normalization and multiplexing, the libraries were sequenced at the University of California Irvine's Genomics Research and Technology Hub on a Illumina NovaSeq 6000 instrument with paired-end chemistry and 150 cycles to achieve ~100 million reads per sample for the combined *P. leucopus*-*M. musculus* experiment. The method for producing cDNA libraries was used for the *R. norvegicus* RNA but these were sequenced on a Illumina HiSeq 4000 instrument with paired-end chemistry and 100 cycles in the same facility. The quality of sequencing reads was analyzed using FastQC (Babraham Bioinformatics). The reads were trimmed of low-quality reads (Phred score of <15) and adapter sequences, and corrected for poor-quality bases using Trimmomatic.

For the combined species experiment the mean (95% confidence interval) number of PE150 reads per animal after trimming for quality was 1.1 (1.0-1.2) x 10^8 for *P. leucopus* and 1.1 (1.0-1.2) x 10^8 for *M. musculus* ($p = 0.91$). For the lower dose-longer duration experiment with *P. leucopus* the mean number of PE150 reads was 2.5 (2.3-2.6) x 10^7. For the rat experiment the mean number of PE100 reads was 2.4 (2.2-2.5) x 10^7.

Genome-wide differential gene expression

Batched fastq files were subjected to analysis with CLC Genomics Workbench version 23 (Qiagen). Library size normalization was done by the TMM (trimmed mean of M values) method of Robinson and Oshlack (Robinson and Oshlack 2010). Differential expression between experimental conditions was assessed with an assumption of a negative binomial distribution for expression level and a separate Generalized Linear Model for each (McCarthy, Chen, and Smyth 2012). Fold changes or differences were $\log_2$-transformed. The False Discovery Rate (FDR) with corrected p value was estimated by the method of Benjamini and Hochberg (Benjamini and Hochberg 1995). The reference genome transcript sets on GenBank were the following: GCF_004664715.2 for *P. leucopus* LL stock, GCF_000001635.27_GRCm39 for *M. musculus* C57Bl/6, and GCF_015227675.2_mRatBN7.2 for *R. norvegicus*. Principal Component Analysis was carried with the "PCA for RNA-Seq" module of the suite of programs; normalization was with *Z*-scores.

For the *P. leucopus* RNA-seq analysis there were 54,466 reference transcripts, of which 48,164 (88%) were mRNAs with protein coding sequences, and 6,302 were identified as non-coding RNAs (ncRNA). Of the 48,164 coding sequences, 40,247 (84%) had matching reads for at least one of the samples. The five most highly represented *P. leucopus* coding sequences among the matched transcripts of whole blood among treated and control animals were hemoglobin subunits alpha and beta, the calprotectin subunits S100A8 and S100A9, and ferritin heavy chain. For the *M. musculus* analysis there were available 130,329 reference transcripts: 92,486 (71%) mRNAs with protein coding sequences and 37,843 ncRNAs. Of the coding sequences, 59,239 (64%) were detectably transcribed in one or both groups by the same criterion. The five most highly represented coding sequences of mRNAs of identified genes for *M. musculus* were hemoglobin subunits alpha and beta, aminolevulinic synthase 2, ferritin light polypeptide 1, and thymosin beta. For *R. norvegicus* there were 99,126 reference transcripts, of which 74,742 (75%) were mRNAs. The five most highly represented coding sequences of mRNAs of identified genes for *R. norvegicus* were hemoglobin subunits alpha and beta, beta-2 microglobulin, ferritin heavy chain, and S100a9.

Gene Ontology term analysis

Enrichment of Gene Ontology (GO; http://geneontology.org) terms for biological processes was computed using EnrichR (https://amp.pharm.mssm.edu/Enrichr) (Chen et al. 2013). *Mus musculus* was selected as the closest reference for the *P. leucopus* and *R. norvegicus* data. The analysis was implemented using the default settings (p value cut-off of 0.01, minimum overlap of 3, and a minmum enrichment of 1.5) of the tools at the Metascape website (https://metascape.org) (Zhou et al. 2019). The GO terms were sorted by ascending p value. Besides the terms beginning with "GO", other terms refer to Kegg Pathway database (https://www.kegg.jp) for "mmu.." designations, WikiPathways database (https://www.wikipathways.org) for "WP…" designations, and Reactome database (https://reactome.org) for "R-MMU…" designations.

Targeted RNA-seq

RNA-seq of selected set of protein coding sequences (CDS), which are listed below, was carried out using CLC Genomics Workbench v. 23 (Qiagen). Paired-end reads were mapped with a length fraction of 0.35 for ~150 nt reads and 0.40 for ~100 nt reads, a similarity fraction of 0.9, and penalties of 3 for mismatch, insertion, or deletion to the CDS of sets of corresponding orthologous mRNAs of *P. leucopus*, *M. musculus*, and *R. norvegicus*. Expression values were unique reads normalized for total reads across all the samples without adjustment for reference sequence length. Exceptions were the endogenous retrovirus coding sequences which differed in lengths between species. These were $\log_{10}$-transformed. For cross-species comparison we normalized for transcripts of a gene, Ptprc or CD45, that is a marker for both granulocytes and mononuclear cells in the blood. The purpose was to adjust for difference in white cell numbers between samples. The Results section provides further details. Following the recommendation of Hedges et al. we used the natural logarithm (*ln*) of ratios (Hedges, Gurevitch, and Curtis 1999). An alternative gene for adjustments for frequencies of white blood cells in the sample was mitochondrial 12S rRNA; mature erythrocytes do not have mitochondria. The coefficient of determination (R^2) for log-transformed fold changes between *Peromyscus* and *Mus* with Ptprc-matched reads for normalization and the corresponding values with mitochondrial 12S rRNA-matched reads for normalization was 0.96 with a coefficient of 1.04. Because of the standard uses of Ptprc/CD45 as a signifier of white blood cells, we chose this gene for indexing over the 12S rRNA.

Target CDS (n=113): Acod1, Akt1, Akt2, Arg1, Bcl3, Camp, Ccl2, Ccl3, Ccl4, Cd14, Cd177, Cd3d, Cd4, Cd69, Cd8, Cfb, Cgas, Csf1, Csf1r, Csf2, Csf3, Csf3r, Cx3cr1, Cxcl1, Cxcl10, Cxcl2, Cxcl3, Dhx58, Fcer2, Fcgr2a, Fcgr2b, Fcgr3 (Cd16), Fgr, Fos, Fpr2, Gapdh, Gbp4, Glrx, Gzmb, Hif1a, Hk3, Hmox1, Ibsp, Icam, Ifih1 (Mda5), Ifit1, Ifng, Il10, Il12, Il18, Il1b, Il1rn, Il2ra, Il4ra, Il6, Il7r, Irf7, Isg15, Itgam (Cd11b), Jak1, Jak2, Jun, Lcn2, Lpo, Lrg, Lrrk2, Ltf, Mapk1, Mmp8, Mmp9, Mpo, MT-Co1, Mt2, Mtor, Mx2, Myc, Myd88, Ncf4, Nfkb1, Ngp, Nos2, Nox1, Nr3c1, Oas1, Olfm4, Padi4, Pbib, Pkm, Ptx, Retn, Rigi (Ddx58), S100a9, Saa3, Serpine1, Slc11a1 (Nramp), Slpi, Socs1, Socs3, Sod2, Stat1, Stat2, Stat4, Steap1, Sting, Tgfb, Thy1, Timp1, Tlr1, Tlr2, Tlr4, Tnf, Tnfrsf1a, and Tnfrsf9. The sources for these coding sequences were the reference genome transcript sets for *P. leucopus, M. musculus*, and *R. norvegicus* listed above under "Genome-wide differential gene expression". If there were two or more isoforms of the mRNAs and the amino acid sequences differed, the default selection for the coding sequence was the first listed isoform. The lengths of the orthologous pairs of *P. leucopus* and *M. musculus* coding sequences were either identical or within 2% of the other. Note that Fcgr1 (Cd64) was not included in the comparison, because in *P. leucopus* it is a pseudogene (GenBank accession OP292976).

Reverse transcriptase-quantitative PCR assays

RT-qPCR assays and the corresponding primers for measurement of transcripts of genes for nitric oxide synthase 2 (Nos2) and glyceraldehyde 3-phosphate dehydrogenase (Gapdh) were those described previously (Balderrama-Gutierrez et al. 2021). These primers worked for M. musculus as well as P. leucopus using modified cycling conditions. For the arginase 1 transcript assays different primer sets were used for each species. The forward and reverse primer sets for the 352 bp Arg1 product for *P. leucopus* were 5′-TCCGCTGACAACCAACTCTG and 5′-GACAGGTGTGCCAGTAGATG, respectively. The corresponding primer pairs for a 348 bp Arg1 of *M. musculus* were 5′-TGTGAAGAACCCACGGTCTG and 5′-ACGTCTCGCAAGCCAATGTA. cDNA synthesis and qPCR were achieved with a Power Sybr Green RNA-to-Ct 1-Step Kit (Applied Biosystems) in 96 MicroAmp Fast Reaction Tubes using an Applied Biosystems StepOne Plus real-time PCR instrument. The initial steps for all assays were 48 °C for 30 min and 95 °C for 10 min. For Arg1 and Nos2 assays, this was followed by 40 cycles of a 2-step PCR of, first, 95°C for 15 s and then, second, annealing and extension at 60 °C for 1 min. The cycling conditions for Gapdh were 40 cycles of 95 °C for 15 s followed by 60 °C for 30 s.

Statistics

Means are presented with asymmetrical 95% confidence intervals (CI) to accommodate data that was not normally distributed. Parametric (*t* test) and non-parametric (Mann-Whitney) tests of significance were 2-tailed. Unless otherwise stated, the *t* test *p* value is given. Categorical variables

were assessed by 2-tailed Fisher's exact test. FDR correction of *p* values for multiple testing was by the Benjamini-Hochberg method (Benjamini and Hochberg 1995), as implemented in CLC Genomics Workbench (see above), or False Discovery Rate Online Calculator (https://tools.carbocation.com/FDR). Discriminant Analysis, linear regression, correlation, coefficient of determination, and General Linear Model analyses were performed with SYSTAT v. 13.1 software (Systat Software, Inc.).

Data availability

The experiments reported here are associated with National Center for Biotechnology Information (https://ncbi.nlm.nih.gov) BioProjects PRJNA975149 for the combined *P. leucopus* and *M. musculus* experiment, PRJNA874306 for the 12 h-lower dose *P. leucopus* experiment, and PRJNA973677 for the *R. norvegicus* LPS experiment. PRJNA975149 includes 40 BioSamples (SAMN35347136-SAMN35347175) and 40 sets of Sequence Read Archive (SRA) fastq files of Illumina paired-end chemistry reads 1 and 2 (SRR24733648-SRR24733687). PRJNA874306 includes 6 BioSamples (SAMN30561752-SAMN30561757) and the corresponding SRA files SRR24451178-SRR24451180, SRR24451183, SRR24451194, and SRR24451195. PRJNA973677 includes 16 BioSamples (SAMN35351370-SAMN35351385) and the corresponding SRA files SRR24731678- SRR24731693. The datasets of the differentially-expressed gene analysis of RNA-seq for the 4 h LPS experiments for *P. leucopus*, *M. musculus*, and *R. norvegicus* are available under the title "In vivo differentially-expressed genes in *Peromyscus leucopus, Mus musculus*, and *Rattus norvegicus* blood in response to LPS" as Table D1 at the public data repository Dryad (https://doi.org/10.7280/D1470Z).

Acknowledgments

We thank Hanjuan Shao for technical assistance, Vanessa Cook for her contribution to the *R. norvegicus* experiment, Anthony Long for identifying in the *P. leucopus* genome candidate endogenous retrovirus sequences, and Brianna Craver-Hoover and Gajalakshmi Ramanathan for blood cell counts performed at U.C. Irvine. The experimental studies reported here were supported by National Institutes of Health (NIH) grants AI-157513 and AI-136523. The services of the Genomics Research and Technology Hub were supported in part by NIH Cancer Center Support Grant P30 CA-062203 and NIH shared instrumentation grants RR-025496, OD-010794, and OD-021718.

REFERENCES

Arranz, A., C. Doxaki, E. Vergadi, Y. Martinez de la Torre, K. Vaporidi, E. D Lagoudaki, E. Ieronymaki, A. Androulidaki, M. Venihaki, and A. N. Margioris. 2012. Akt1 and Akt2 protein kinases differentially contribute to macrophage polarization. *Proc Natl Acad Sci U S A* 109 (24): 9517-9522.

Balderrama-Gutierrez, G., A. Milovic, V. J. Cook, M. N. Islam, Y. Zhang, H. Kiaris, J. T. Belisle, A. Mortazavi, and A. G. Barbour. 2021. An infection-tolerant mammalian reservoir for several zoonotic agents broadly counters the inflammatory effects of endotoxin. *mBio* 12 (2). https://doi.org/10.1128/mBio.00588-21.

Barbour, A. G. 2017. Infection resistance and tolerance in *Peromyscus* spp., natural reservoirs of microbes that are virulent for humans. *Semin Cell Dev Biol* 61 (1): 115-122. https://doi.org/10.1016/j.semcdb.2016.07.002.

Barbour, A. G., H. Shao, V. J. Cook, J. Baldwin-Brown, J. I. Tsao, and A. D. Long. 2019. Genomes, expression profiles, and diversity of mitochondria of the white-footed deermouse Peromyscus leucopus, reservoir of Lyme disease and other zoonoses. *Sci Rep* 9 (1): 17618. https://doi.org/10.1038/s41598-019-54389-3.

Bedford, N. L., and H. E. Hoekstra. 2015. Peromyscus mice as a model for studying natural variation. *Elife* 4: e06813. https://doi.org/10.7554/eLife.06813.

Benjamini, Yoav, and Yosef Hochberg. 1995. Controlling the false discovery rate: a practical and powerful approach to multiple testing. *J Roy Stat Soc. Series B (Methodological)*: 57(1): 289-300.

Biser, J. A., L. A. Vogel, J. Berger, B. Hjelle, and S. S. Loew. 2004. Effects of heavy metals on immunocompetence of white-footed mice (Peromyscus leucopus). *J Wildl Dis* 40 (2): 173-84. https://doi.org/10.7589/0090-3558-40.2.173.

Bothwell, A., P. E. Pace, and K. P. LeClair. 1988. Isolation and expression of an IFN-responsive Ly-6C chromosomal gene. *J Immunol* 140 (8): 2815-20.

Botten, J., K. Mirowsky, D. Kusewitt, M. Bharadwaj, J. Yee, R. Ricci, R. M. Feddersen, and B. Hjelle. 2000. Experimental infection model for Sin Nombre hantavirus in the deer mouse (Peromyscus maniculatus). *Proc Natl Acad Sci U S A* 97 (19): 10578-83. https://doi.org/10.1073/pnas.180197197.

Bradley, R.D., L.K, Ammerman, R.J. Baker, L.C. Bradley, J.A. Cook, R.C. Dowler, C. Jones, D.J. Schmidly, F.B. Stangl, and R.A. Van Den Bussche. 2014. *Revised checklist of North American mammals north of Mexico, 2014*. Museum of Texas Tech University.

Bunikis, J., J. Tsao, C. J. Luke, M. G. Luna, D. Fish, and A. G. Barbour. 2004. Borrelia burgdorferi infection in a natural population of Peromyscus leucopus mice: a longitudinal study in an area where Lyme Borreliosis is highly endemic. *J Infect Dis* 189 (8): 1515-23. https://doi.org/10.1086/382594

Chable-Santos, J. B., N. R. Van Wynsberghe, S. B. Canto-Lara, and F. J. Andrade-Narvaez. 1995. Isolation of Leishmania (L.) mexicana from wild rodents and their possible role in the transmission of localized cutaneous leishmaniasis in the state of Campeche, Mexico. *Am J Trop Med Hyg* 53 (2): 141-5. https://doi.org/10.4269/ajtmh.1995.53.141.

Charles River. 2012. CD-1 Mouse Hematology. Charles River. Accessed March 30, 2023. https://www.criver.com/sites/default/files/resources/doc_a/CD-1MouseClinicalPathologyData.pdf.

Chen, E. Y., C. M. Tan, Y. Kou, Q. Duan, Z. Wang, G. V. Meirelles, N. R. Clark, and A. Ma'ayan. 2013. Enrichr: interactive and collaborative HTML5 gene list enrichment analysis tool. *BMC Bioinformatics* 14: 128. https://doi.org/10.1186/1471-2105-14-128.

Chiaranunt, P., K. Burrows, L. Ngai, E. Y. Cao, H. Liang, S. L. Tai, C. J. Streutker, S. E. Girardin, and A. Mortha. 2022. NLRP1B and NLRP3 Control the Host Response following Colonization with the Commensal Protist Tritrichomonas musculis. *J Immunol* 208 (7): 1782-1789. https://doi.org/10.4049/jimmunol.2100802.

Childs, J. E., T. G. Ksiazek, C. F. Spiropoulou, J. W. Krebs, S. Morzunov, G. O. Maupin, K. L. Gage, P. E. Rollin, J. Sarisky, R. E. Enscore, and et al. 1994. Serologic and genetic identification of Peromyscus maniculatus as the primary rodent reservoir for a new hantavirus in the southwestern United States. *J Infect Dis* 169 (6): 1271-80.

Coburn, Jenifer, Brandon Garcia, Linden T Hu, Mollie W Jewett, Peter Kraiczy, Steven J Norris, and Jon Skare. 2021. Lyme disease pathogenesis. *Current Issues Mol Biol* 42 (1): 473-518.

Cook, V., and A. G. Barbour. 2015. Broad diversity of host responses of the white-footed mouse Peromyscus leucopus to Borrelia infection and antigens. *Ticks Tick Borne Dis* 6 (5): 549-58. https://doi.org/10.1016/j.ttbdis.2015.04.009.

De Cecco, M., T. Ito, A.P. Petrashen, A.E. Elias, N.J. Skvir, S.W. Criscione, A. Caligiana, G. Brocculi, E.M. Adney, J.D. Boeke, O. Le, C. Beauséjour, J. Ambati, K. Ambati, M. Simon, A. Seluanov, V. Gorbunova, P. E. Slagboom, S.L. Helfand, N.Neretti, and J.M. Sedivy. 2019. L1 drives IFN in senescent cells and promotes age-associated inflammation. *Nature* 566 (7742): 73-78. https://doi.org/10.1038/s41586-018-0784-9.

Deschambault, Y., L. Klassen, G. Soule, K. Tierney, K. Azaransky, A. Sloan, and D. Safronetz. 2023. Experimental Infection of North American Deer Mice with Clade I and II Monkeypox Virus Isolates. *Emerg Infect Dis* 29 (4): 858-860. https://doi.org/10.3201/eid2904.221594.

Diuk-Wasser, M. A., A. G. Hoen, P. Cislo, R. Brinkerhoff, S. A. Hamer, M. Rowland, R. Cortinas, G. Vourc'h, F. Melton, G. J. Hickling, J. I. Tsao, J. Bunikis, A. G. Barbour, U. Kitron, J. Piesman, and D. Fish. 2012. Human risk of infection with Borrelia burgdorferi, the Lyme disease agent, in eastern United States. *Am J Tropl Med Hyg* 86 (2): 320-7. https://doi.org/10.4269/ajtmh.2012.11-0395.

Escalante, N. K., P. Lemire, M. Cruz Tleugabulova, D. Prescott, A. Mortha, C. J. Streutker, S. E. Girardin, D. J. Philpott, and T. Mallevaey. 2016. The common mouse protozoa Tritrichomonas muris alters mucosal T cell homeostasis and colitis susceptibility. *J Exp Med* 213 (13): 2841-2850. https://doi.org/10.1084/jem.20161776.

Fagre, A., J. Lewis, M. Eckley, S. Zhan, S. M. Rocha, N. R. Sexton, B. Burke, B. Geiss, O. Peersen, T. Bass, R. Kading, J. Rovnak, G. D. Ebel, R. B. Tjalkens, T. Aboellail, and T. Schountz. 2021. SARS-CoV-2 infection, neuropathogenesis and transmission among deer mice: Implications for spillback to New World rodents. *PLoS Pathog* 17 (5): e1009585. https://doi.org/10.1371/journal.ppat.1009585.

Griffin, B. D., M. Chan, N. Tailor, E. J. Mendoza, A. Leung, B. M. Warner, A. T. Duggan, E. Moffat, S. He, L. Garnett, K. N. Tran, L. Banadyga, A. Albietz, K. Tierney, J. Audet, A. Bello, R. Vendramelli, A. S. Boese, L. Fernando, L. R. Lindsay, C. M. Jardine, H. Wood, G. Poliquin, J. E. Strong, M. Drebot, D. Safronetz, C. Embury-Hyatt, and D. Kobasa. 2021. SARS-CoV-2 infection and transmission in the North American deer mouse. *Nat Commun* 12 (1): 3612. https://doi.org/10.1038/s41467-021-23848-9.

Hall, E.R. 1979. *Mammals of North America*. 2 vols. Vol. 2. New York, NY: John Wiley and Sons.

Hara, I., S. Izui, P. J. McConahey, J. H. Elder, F. C. Jensen, and F. J. Dixon. 1981. Induction of high serum levels of retroviral env gene products (gp70) in mice by bacterial lipopolysaccharide. *Proc Natl Acad Sci U S A* 78 (7): 4397-401. https://doi.org/10.1073/pnas.78.7.4397.

Hedges, L.V., J. Gurevitch, and P.S. Curtis. 1999. The meta-analysis of response ratios in experimental ecology. *Ecology* 80 (4): 1150-1156.

Heinzelmann, Michael, Hiram C Polk Jr, Alexander Chernobelsky, Thomas P Stites, and Laura E Gordon. 2000. Endotoxin and muramyl dipeptide modulate surface receptor expression on human mononuclear cells. *Immunopharmacology* 48 (2): 117-128.

Hoen, A. G., G. Margos, S. J. Bent, M. A. Diuk-Wasser, A. Barbour, K. Kurtenbach, and D. Fish. 2009. Phylogeography of Borrelia burgdorferi in the eastern United States reflects multiple independent Lyme disease emergence events. *Proc Natl Acad Sci U S A* 106 (35): 15013-8. https://doi.org/10.1073/pnas.0903810106. http://www.ncbi.nlm.nih.gov/pubmed/19706476.

Hurst, T. P., and G. Magiorkinis. 2015. Activation of the innate immune response by endogenous retroviruses. *J Gen Virol* 96 (Pt 6): 1207-1218. https://doi.org/10.1099/jgv.0.000017.

Italiani, P., and D. Boraschi. 2014. From Monocytes to M1/M2 Macrophages: Phenotypical vs. Functional Differentiation. *Front Immunol* 5: 514. https://doi.org/10.3389/fimmu.2014.00514.

Jongstra, J., and C. Moroni. 1981. Lipopolysaccharide induces retroviral antigen expression in 129/J mouse lymphocytes: evidence for assembly of a defective viral particle. *J Virol* 37 (3): 1044-50. https://doi.org/10.1128/jvi.37.3.1044-1050.1981.

Joyner, C. P., L. C. Myrick, J. P. Crossland, and W. D. Dawson. 1998. Deer mice as laboratory animals. *ILAR* 39 (4): 322-330. http://www.ncbi.nlm.nih.gov/pubmed/11406688.

Kong, L., L. Sun, H. Zhang, Q. Liu, Y. Liu, L. Qin, G. Shi, J. H. Hu, A. Xu, Y. P. Sun, D. Li, Y. F. Shi, J. W. Zang, J. Zhu, Z. Chen, Z. G. Wang, and B. X. Ge. 2009. An essential role for RIG-I in toll-like receptor-stimulated phagocytosis. *Cell Host Microbe* 6 (2): 150-61. https://doi.org/10.1016/j.chom.2009.06.008.

Kuroda, Etsushi, Tomohiro Kito, and Uki Yamashita. 2002. Reduced expression of STAT4 and IFN-γ in macrophages from BALB/c mice. *J Immunol* 168 (11): 5477-5482.

Labinskyy, N., P. Mukhopadhyay, J. Toth, G. Szalai, M. Veres, G. Losonczy, J. T. Pinto, P. Pacher, P. Ballabh, A. Podlutsky, S. N. Austad, A. Csiszar, and Z. Ungvari. 2009. Longevity is associated with increased vascular resistance to high glucose-induced oxidative stress and inflammatory gene expression in Peromyscus leucopus. *Am J Physiol Heart Circ Physiol* 296 (4): H946-56. https://doi.org/10.1152/ajpheart.00693.2008.

Langeroudi, A. G., C. M. Hirsch, A. S. Estabragh, S. Meinardi, D. R. Blake, and A. G. Barbour. 2014. Elevated carbon monoxide to carbon dioxide ratio in the exhaled breath of mice treated with a single dose of lipopolysaccharide. *Open Forum Infect Dis* 1 (2): ofu085. https://doi.org/10.1093/ofid/ofu085.

Levengood, J. M., and E. J. Heske. 2008. Heavy metal exposure, reproductive activity, and demographic patterns in white-footed mice (Peromyscus leucopus) inhabiting a contaminated floodplain wetland. *Sci Total Environ* 389 (2-3): 320-8. https://doi.org/10.1016/j.scitotenv.2007.08.050.

Lima-Junior, D. S., S. R. Krishnamurthy, N. Bouladoux, N. Collins, S. J. Han, E. Y. Chen, M. G. Constantinides, V. M. Link, A. I. Lim, M. Enamorado, C. Cataisson, L. Gil, I. Rao, T. K. Farley, G. Koroleva, J. Attig, S. H. Yuspa, M. A. Fischbach, G. Kassiotis, and Y. Belkaid. 2021. Endogenous retroviruses promote homeostatic and inflammatory responses to the microbiota. *Cell* 184 (14): 3794-3811.e19. https://doi.org/10.1016/j.cell.2021.05.020.

Long, A.L., J. Baldwin-Brown, Y. Tao, V.J. Cook, G. Balderrama-Gutierrez, R. Corbett-Detig, A. Mortazavi, and A.G. Barbour. 2019. The genome of Peromyscus leucopus, natural host for Lyme disease and other emerging infections. *Sci Advances* 5 (7): eaaw6441. https://doi.org/10.1126/sciadv.aaw6441.

Long, P. N., V. J. Cook, A. Majumder, A. G. Barbour, and A. D. Long. 2022. The utility of a closed breeding colony of Peromyscus leucopus for dissecting complex traits. *Genetics* 221 (1). https://doi.org/10.1093/genetics/iyac026.

Loría-Cervera, E. N., E. I. Sosa-Bibiano, N. R. Van Wynsberghe, and F. J. Andrade-Narváez. 2018. Finding a model for the study of Leishmania (Leishmania) mexicana infection: The Yucatan Deer mouse (Peromyscus yucatanicus) as a suitable option. *Acta Trop* 187: 158-164. https://doi.org/10.1016/j.actatropica.2018.08.003.

Lowenstein, C. J., E. W. Alley, P. Raval, A. M. Snowman, S. H. Snyder, S. W. Russell, and W. J. Murphy. 1993. Macrophage nitric oxide synthase gene: two upstream regions mediate induction by interferon gamma and lipopolysaccharide. *Proc Natl Acad Sci U S A* 90 (20): 9730-4.

MacMicking, J.D., C. Nathan, G. Hom, N. Chartrain, D.S. Fletcher, M. Trumbauer, K. Stevens, Q-W. Xie, K. Sokol, N. Hutchinson, H. Chen, and J.S. Mudget. 1995. Altered responses to bacterial infection and endotoxic shock in mice lacking inducible nitric oxide synthase. *Cell* 81 (4): 641-650. https://doi.org/10.1016/0092-8674(95)90085-3.

Mandl, J. N., C. Schneider, D. S. Schneider, and M. L. Baker. 2018. Going to Bat(s) for Studies of Disease Tolerance. *Front Immunol* 9: 2112. https://doi.org/10.3389/fimmu.2018.02112.

Mazgaeen, L., and P. Gurung. 2020. Recent Advances in Lipopolysaccharide Recognition Systems. *Int J Mol Sci* 21 (2). https://doi.org/10.3390/ijms21020379.

McCarthy, D.J., Y. Chen, and G.K. Smyth. 2012. Differential expression analysis of multifactor RNA-Seq experiments with respect to biological variation. *Nucleic Acids Res* 40 (10): 4288-4297. https://doi.org/10.1093/nar/gks042.

McClure, M., and S. Kaye. 2010. Can detection of xenotropic murine leukemia virus-related virus be linked to chronic fatigue syndrome? *Exp Rev Mol Diagnostics* 10 (5): 537-539.

Milovic, A, J.V. Duong, J. Gach, I. Chatzistamou, T. Lane, D.N. Forthal, and A.G. Barbour. 2023. SARS-CoV-2 virus infection of lungs and brain of the white-footed deermouse Peromyscus leucopus. *Manuscript in preparation*.

Milovic, A., K. Bassam, H. Shao, I. Chatzistamou, D. M. Tufts, M. Diuk-Wasser, and A. G. Barbour. 2020. Lactobacilli and other gastrointestinal microbiota of Peromyscus leucopus, reservoir host for agents of Lyme disease and other zoonoses in North America. *PLoS One* 15 (8): e0231801. https://doi.org/10.1371/journal.pone.0231801.

Mlera, L., K. Meade-White, G. Saturday, D. Scott, and M. E. Bloom. 2017. Modeling Powassan virus infection in Peromyscus leucopus, a natural host. *PLoS Negl Trop Dis* 11 (1): e0005346. https://doi.org/10.1371/journal.pntd.0005346.

Mommert, M., O. Tabone, A. Guichard, G. Oriol, E. Cerrato, M. Denizot, V. Cheynet, A. Pachot, A. Lepape, G. Monneret, F. Venet, K. Brengel-Pesce, J. Textoris, and F. Mallet. 2020. Dynamic LTR retrotransposon transcriptome landscape in septic shock patients. *Crit Care* 24 (1): 96. https://doi.org/10.1186/s13054-020-2788-8.

Moody, K. D., G. A. Terwilliger, G. M. Hansen, and S. W. Barthold. 1994. Experimental Borrelia burgdorferi infection in Peromyscus leucopus. *J Wildl Dis* 30 (2): 155-61. https://doi.org/10.7589/0090-3558-30.2.155.

Morzunov, S. P., J. E. Rowe, T. G. Ksiazek, C. J. Peters, S. C. St Jeor, and S. T. Nichol. 1998. Genetic analysis of the diversity and origin of hantaviruses in Peromyscus leucopus mice in North America. *J Virol* 72 (1): 57-64.

Moscarella, R.A., S.M.G Hoffman, P. Myers, C. J. Yahnke, and B.L Lundrigan. 2019. Genetic and demographic analysis of invasive Peromyscus leucopus in the northern Great Lakes region. *J Mammalogy* 100 (2): 345-353. https://doi.org/10.1093/jmammal/gyz053. https://doi.org/10.1093/jmammal/gyz053.

Munshi-South, J., and K. Kharchenko. 2010. Rapid, pervasive genetic differentiation of urban white-footed mouse (Peromyscus leucopus) populations in New York City. *Mol Ecol*. https://doi.org/10.1111/j.1365-294X.2010.04816.x.

Murray, P. J., J. E. Allen, S. K. Biswas, E. A. Fisher, D. W. Gilroy, S. Goerdt, S. Gordon, J. A. Hamilton, L. B. Ivashkiv, T. Lawrence, M. Locati, A. Mantovani, F. O. Martinez, J. L. Mege, D. M. Mosser, G. Natoli, J. P. Saeij, J. L. Schultze, K. A. Shirey, A. Sica, J. Suttles, I. Udalova, J. A. van Ginderachter, S. N. Vogel, and T. A. Wynn. 2014. Macrophage activation and polarization: nomenclature and experimental guidelines. *Immunity* 41 (1): 14-20. https://doi.org/10.1016/j.immuni.2014.06.008.

Murray, P. J. 2017. Macrophage polarization. *Ann Rev Physiol* 79: 541-566.

Narasimhan, P. B., P. Marcovecchio, A. A. J. Hamers, and C. C. Hedrick. 2019. Nonclassical Monocytes in Health and Disease. *Annu Rev Immunol* 37: 439-456. https://doi.org/10.1146/annurev-immunol-042617-053119.

Nathan, C. 2022. Nonresolving inflammation redux. *Immunity* 55 (4): 592-605. https://doi.org/10.1016/j.immuni.2022.03.016.

Norgard, M. V., L. L. Arndt, D. R. Akins, L. L. Curetty, D. A. Harrich, and J. D. Radolf. 1996. Activation of human monocytic cells by Treponema pallidum and Borrelia burgdorferi lipoproteins and synthetic lipopeptides proceeds via a pathway distinct from that of lipopolysaccharide but involves the transcriptional activator NF-kappa B. *Infect Immun* 64 (9): 3845-52. https://doi.org/10.1128/iai.64.9.3845-3852.1996.

Pisano, M. P., O. Tabone, M. Bodinier, N. Grandi, J. Textoris, F. Mallet, and E. Tramontano. 2020. RNA-Seq Transcriptome Analysis Reveals Long Terminal Repeat Retrotransposon Modulation in Human Peripheral Blood Mononuclear Cells after In Vivo Lipopolysaccharide Injection. *J Virol* 94 (19). https://doi.org/10.1128/jvi.00587-20.

Quatrini, L., E. Wieduwild, S. Guia, C. Bernat, N. Glaichenhaus, E. Vivier, and S. Ugolini. 2017. Host resistance to endotoxic shock requires the neuroendocrine regulation of group 1 innate lymphoid cells. *J Exp Med* 214 (12): 3531-3541. https://doi.org/10.1084/jem.20171048.

Rangel, S. C., M. D. da Silva, A. L. da Silva, J. M. B. Dos Santos, L. M. Neves, A. Pedrosa, F. M. Rodrigues, C. D. S. Trettel, G. E. Furtado, M. P. de Barros, A. L. L. Bachi, C. M. Romano, and Lhds Nali. 2022. Human endogenous retroviruses and the inflammatory response: A vicious circle associated with health and illness. *Front Immunol* 13: 1057791. https://doi.org/10.3389/fimmu.2022.1057791.

Robinson, M. D., and A. Oshlack. 2010. A scaling normalization method for differential expression analysis of RNA-seq data. *Genome Biol* 11 (3): R25. https://doi.org/10.1186/gb-2010-11-3-r25.

Russ, E., and S. Iordanskiy. 2023. Endogenous retroviruses as modulators of innate immunity. *Pathogens* 12 (2): 162.

Sacher, G. A., and R. W. Hart. 1978. Longevity, aging and comparative cellular and molecular biology of the house mouse, Mus musculus, and the white-footed mouse, Peromyscus leucopus. *Birth Defects Orig Artic Ser* 14 (1): 71-96.

Salazar, J. C., S. Duhnam-Ems, C. La Vake, A. R. Cruz, M. W. Moore, M. J. Caimano, L. Velez-Climent, J. Shupe, W. Krueger, and J. D. Radolf. 2009. Activation of human monocytes by live Borrelia burgdorferi generates TLR2-dependent and -independent responses which include

induction of IFN-beta. *PLoS Pathog* 5 (5): e1000444. https://doi.org/10.1371/journal.ppat.1000444.
Salkowski, C. A., G. Detore, R. McNally, N. van Rooijen, and S. N. Vogel. 1997. Regulation of inducible nitric oxide synthase messenger RNA expression and nitric oxide production by lipopolysaccharide in vivo: the roles of macrophages, endogenous IFN-gamma, and TNF receptor-1-mediated signaling. *J Immunol* 158 (2): 905-12.
Schnizlein-Bick, C. T., F. F. Mandy, M. R. O'Gorman, H. Paxton, J. K. Nicholson, L. E. Hultin, R. S. Gelman, C. L. Wilkening, and D. Livnat. 2002. Use of CD45 gating in three and four-color flow cytometric immunophenotyping: guideline from the National Institute of Allergy and Infectious Diseases, Division of AIDS. *Cytometry* 50 (2): 46-52. https://doi.org/10.1002/cyto.10073.
Schwanz, L. E., M. J. Voordouw, D. Brisson, and R. S. Ostfeld. 2011. Borrelia burgdorferi has minimal impact on the Lyme disease reservoir host Peromyscus leucopus. *Vector Borne Zoonotic Dis* 11 (2): 117-24. https://doi.org/10.1089/vbz.2009.0215.
Soudi, S., A. Zavaran-Hosseini, Z. M. Hassan, M. Soleimani, F. J. Adegani, and S. Mahmoud Hashemi. 2013. Comparative study of the effect of LPS on the function of BALB/c and C57BL/6 peritoneal macrophages. *Cell Journal (Yakhteh)* 15 (1): 45-54.
Steere, A. C., N. H. Bartenhagen, J. E. Craft, G. J. Hutchinson, J. H. Newman, A. R. Pachner, D. W. Rahn, L. H. Sigal, E. Taylor, and S. E. Malawista. 1986. Clinical manifestations of Lyme disease. *Zentralbl Bakteriol Mikrobiol Hyg [A]* 263 (1-2): 201-5.
Steere, A. C., V. K. Sikand, F. Meurice, D. L. Parenti, E. Fikrig, R. T. Schoen, J. Nowakowski, C. H. Schmid, S. Laukamp, C. Buscarino, and D. S. Krause. 1998. Vaccination against Lyme disease with recombinant Borrelia burgdorferi outer-surface lipoprotein A with adjuvant. Lyme Disease Vaccine Study Group. *N Engl J Med* 339 (4): 209-15.
Stoye, J. P., and C. Moroni. 1983. Endogenous retrovirus expression in stimulated murine lymphocytes. Identification of a new locus controlling mitogen induction of a defective virus. *J Exp Med* 157 (5): 1660-74. https://doi.org/10.1084/jem.157.5.1660.
van Stijn, C. M., J. Kim, A. J. Lusis, G. D. Barish, and R. K. Tangirala. 2015. Macrophage polarization phenotype regulates adiponectin receptor expression and adiponectin anti-inflammatory response. *Faseb j* 29 (2): 636-49. https://doi.org/10.1096/fj.14-253831.
Vergadi, E., E. Ieronymaki, K. Lyroni, K. Vaporidi, and C. Tsatsanis. 2017. Akt signaling pathway in macrophage activation and M1/M2 polarization. *J Immunol* 198 (3): 1006-1014.
Voordouw, M. J., S. Lachish, and M. C. Dolan. 2015. The Lyme disease pathogen has no effect on the survival of its rodent reservoir host. *PLoS One* 10 (2): e0118265. https://doi.org/10.1371/journal.pone.0118265.
Wei, X. Q., I. G. Charles, A. Smith, J. Ure, G. J. Feng, F. P. Huang, D. Xu, W. Muller, S. Moncada, and F. Y. Liew. 1995. Altered immune responses in mice lacking inducible nitric oxide synthase. *Nature* 375 (6530): 408-11. https://doi.org/10.1038/375408a0.
Wiedmeyer, C. E., J. P. Crossland, M. Veres, M. J. Dewey, M. R. Felder, S. C. Barlow, P. B. Vrana, and G. Szalai. 2014. Hematologic and serum biochemical values of 4 species of Peromyscus mice and their hybrids. *J Am Assoc Lab Anim Sci* 53 (4): 336-43.
Wolf, G., P. Yang, A. C. Füchtbauer, E. M. Füchtbauer, A. M. Silva, C. Park, W. Wu, A. L. Nielsen, F. S. Pedersen, and T. S. Macfarlan. 2015. The KRAB zinc finger protein ZFP809 is required to initiate epigenetic silencing of endogenous retroviruses. *Genes Dev* 29 (5): 538-54. https://doi.org/10.1101/gad.252767.114.
Xiao, W., M. N. Mindrinos, J. Seok, J. Cuschieri, A. G. Cuenca, H. Gao, D. L. Hayden, L. Hennessy, E. E. Moore, J. P. Minei, P. E. Bankey, J. L. Johnson, J. Sperry, A. B. Nathens, T. R. Billiar, M. A. West, B. H. Brownstein, P. H. Mason, H. V. Baker, C. C. Finnerty, M. G. Jeschke, M. C. López, M. B. Klein, R. L. Gamelli, N. S. Gibran, B. Arnoldo, W. Xu, Y. Zhang, S. E. Calvano, G. P. McDonald-Smith, D. A. Schoenfeld, J. D. Storey, J. P. Cobb, H. S. Warren, L. L. Moldawer, D. N. Herndon, S. F. Lowry, R. V. Maier, R. W. Davis, and R. G. Tompkins. 2011. A genomic

storm in critically injured humans. *J Exp Med* 208 (13): 2581-90. https://doi.org/10.1084/jem.20111354.
Zhou, Y., B. Zhou, L. Pache, M. Chang, A. H. Khodabakhshi, O. Tanaseichuk, C. Benner, and S. K. Chanda. 2019. Metascape provides a biologist-oriented resource for the analysis of systems-level datasets. *Nat Commun* 10 (1): 1523. https://doi.org/10.1038/s41467-019-09234-6.

List of Supplementary Materials

Figure S1. Scatter plots of log-transformed normalized transcripts of interleukin-1 beta or nitric oxide synthase 2 on interferon-gamma of blood of *P. leucopus* or *M. musculus* (CD-1 or BALB/c) with or without treatment with lipopolysaccharide

Table S1. High ranking differentially-expressed genes in genome-wide RNA-seq of blood of *P. leucopus* LL stock and *M. musculus* CD-1 with and without treatment with lipopolysaccharide. Excel format (.xlsx) spreadsheet.

Table S2. Individual normalized values for targeted RNA-seq summarized in Table 2 for *P. leucopus* and *M. musculus* with and without treatment with lipopolysaccharide. The table also includes animal identifications, sex of animals., and Akt1/Akt2, Cd14/Cd16 (Fcgr3), Ifng/Il1b, Il12/Il10, and Nos2/Arg1 ratios of reads. First row is table description. Spreadsheet in .csv format.